Rotational Raman Scattering in Exoplanet Atmospheres

Arthur Baartmans

June 8, 2012

Abstract

Since the discovery of the first exoplanets in the 1990's attempts have been made to learn more about these planets than just their orbital parameters and radius or minimum mass. We make use of the fact that star light is generally unpolarized whereas light reflected of planets is polarized due to scattering in the atmosphere. Specifically modelled are the effects of Rotational Raman scattering, a non-elastic form of scattering, to see if its effects are visible in the combined spectrum of the star and planet. The results are discussed and ways to improve the models are proposed.

Contents

1 Introduction

1.1 Exoplanets

Since the discovery of 51 Peg-b, the first planet around a main sequence star other than the Sun in 1995 (Mayor & Queloz (1995) [1]), on the order of 600 exoplanets have been discovered using a variety of, usually indirect, methods. Characterizing exoplanets is more difficult than finding them. Chief reason for this is the fact that even a Jupiter sized planet orbiting close to its parent star will generally reflect less than 0.1% of the light radiated by the parent star. Rodler et al (2010) [2] failed to detect light reflected of the planet τ Boo-b. From this they concluded that the planet has a geometric albedo less than 0.4 assuming a radius of $1.2R_{\text{Jupiter}}$.

1.2 The Ring effect and Raman scattering

Grainger & Ring (1962) [3] found that the calcium H line in the spectrum of reflected sunlight in the Earth's atmosphere is less deep than the same line in unscattered light, this phenomenon has since become know as the Ring effect. Noxon & Goody (1965) [4] repeated the observations by Grainger & Ring (1962) [3], which they confirmed. They also found that the light inside the strong Fraunhofer lines has a degree of polarization less than the continuum degree of polarization. It has since become clear that this phenomenon is caused by Raman scattering of light in the Earth atmosphere (see Stam et al. (2002) [5] and references therein). The filling of the lines by the non-elastic Raman scattering means that the spectral lines in the reflected spactra will have a lower degree of polarization than the surrounding continuum. It is specifically this effect that we have simulated for exoplanet atmospheres, in order to determine if it is possible to detect Raman scattered light or an exoplanet in a star's polarized spectrum. For this we used an adapted version of the code used by Stam et al. (2002) [5].

1.3 Polarimetry in solar system

Measurements of the polarized spectra, including Raman scattering, have been made for the gas giants in our own solar system. Bétremieux & Yelle (1999) [6] used HST data to detect Raman scattering in the Jovian atmosphere. Polarization measurements of the other gas giant have been done by, for example, Sromovsky (2005) [7]. The methods used by Sromovsky and Bétremieux & Yelle differ from the method used here. Further, because the gas giants in the solar system can be resolved, it is possible to observe the effect of Raman scattering at different points on the planet. For exoplanets, even if they could be seen directly, this is not the case, therefore it is necessary to integrate the reflected starlight over the entire visible part of the planet.

Section 2 describes polarized light in general and Raman scattering in particular, section 3 describes the various geometries involved in the problem and how to calculate needed angle from them, section 4 describes a method for integration over a disk, section 5 describes how the spectrum depends on various atmospheric parameters and section 6 describes the dependence on angle of the spectrum. In section 7 the results from the simulations will be presented, a final discussion and conclusion can be found in section 8.

2 Polarized Light

2.1 Describing Polarized Light

2.1.1 The Stokes' vector

Polarized light relative to a given reference plane is normally described using the Stokes' vector $I(\vec{\lambda})$ where

$$\vec{I} = \begin{pmatrix} I(\lambda) \\ Q(\lambda) \\ U(\lambda) \\ V(\lambda) \end{pmatrix} \tag{1}$$

Here $I(\lambda)$ is the total intensity at wavelength λ, $Q(\lambda)$ is linear polarization in the local x or y direction, $U(\lambda)$ is linear polarization at an angle of 45° relative to the x direction and $V(\lambda)$ is the circular polarization.

2.1.2 Changing between reference planes.

The used code calculates I and Q relative to the local meridian plane, that is the plane containing the vector of the incoming light and the vector of the local zenith. However the values for I, Q and U for the planet as a whole are relative to the planetary scattering plane, which is the plane containing the center of the star, the center planet and the observer. Further the planetary scattering plane is generally not the same as the optical plane. To transform the Stokes' parameters found in one plane of reference to another plane of reference one can use the rotation matrix $\mathbf{L}$, such that $\vec{I_{\text{new}}} = \mathbf{L} \cdot \vec{I_{\text{old}}}$. The rotation matrix $\mathbf{L}$ is defined as:

$$\mathbf{L} = \begin{pmatrix} 1 & 0 & 0 & 0 \\ 0 & \cos 2\beta & \sin 2\beta & 0 \\ 0 & -\sin 2\beta & \cos 2\beta & 0 \\ 0 & 0 & 0 & 1 \end{pmatrix} \tag{2}$$

The angle β is the angle between the old and the new plane measured in the counterclockwise direction, with $\beta \geq 0$. An expression for β for any point on the planet can be found in equation 24, section 3.

2.2 Raman Scattering

Raman Scattering is one, non-elastic, of two kinds of scattering that together make up what is generally called Rayleigh scattering. The other, elastic, kind is Cabannes scattering. To confuse matters Cabannes scattering is often simply called Rayleigh scattering. This is because usually when Rayleigh scattering is used in models, scattering is assumed to be fully elastic. However to get a proper model of the effect of scattering non-elastic, i.e. Raman, scattering must also be taken into account. Because Raman scatttering is non-elasctic it allows flux to move between wavelengths, this will cause absorbation lines in the normal, unpolarized, spectrum of an object to be partially filled in. An effect of this filling in is that whereas an absorbtion line will not show up in a polarzation spectrum using only elastic scattering, it will show up in a spectrum where non-elasctic scattering is included because the total flux in the line will have increased while only the original flux will be partially polarized. A short discussion about different nomenclature in Rayleigh scattering can be found in Young (1981) [8].

2.2.1 Scattering Fraction

It is usual to denote the fraction of Cabannes scattered light, relative to the total of the Rayleigh scatter light, with f and consequently the fraction of Raman scattered light by $1 - f$. The fraction f is calculated from the anisotropy factor ϵ using (Stam et al. (2002) [5]):

$$f = \frac{18 + \epsilon(\lambda)}{18 + 4\epsilon(\lambda)} \tag{3}$$

The anisotropy factor can be calculated using either the depolarization factor, ρ or the King correction factor F_{K}, using (Stam et al. (2002) [5],Sneep & Ubachs (2005) [9])

$$\epsilon = \frac{45\rho}{6 - 7\rho} = \frac{9}{2}[F_{\text{K}} - 1] \tag{4}$$

Because the code uses both ρ and F_{K} it is useful to rewrite equation 4 to:

$$\rho = 6\frac{F_{\mathrm{K}} - 1}{7F_{\mathrm{K}} + 3} \tag{5}$$

2.2.2 Strength of the lines

A photon being scattered by a molecule in a state characterize by the rotational-angular-momentum quantum number J, can be Raman scattered to either the $J-2$ or the $J+2$ state (Penney et al. (1973) [10]). The corresponding shift in wavenumber, given in cm^{-1} is then equal to $-(4J+6)B_0$ for $J \rightarrow J+2$ and $(4J-2)B_0$ for $J \rightarrow J-2$ [10]. B_0 is the rotational constant for the lowest vibrational level and has unit cm^{-1}. The fraction of molecule in a state J, F_J is given by Penney et al. (1973) [10]:

$$F_J = Q^{-1} g_J (2J+1) \exp(-E_J/kT) \tag{6}$$

Where g_J is a statistical weight factor, kT is the Boltzmann constant multiplied by the temperature, E_J is the rotational energy, which is approximately equal to $E_J = J(J+1)hcB_0$ en Q is a normalization factor such that $\sum_{J=1}^{\infty} F_J = 1$. Tabel 1 gives an overview of F_{K}, ρ, g_j and B_0 for the molecules used in the models, including a wavelength interval for which they were reported.

It should be noted that the values reported in Tabel 1 have all been experimentally determined for either $T = 273\mathrm{K}$ or $T = 300\mathrm{K}$ with no temperature dependence given. Because we didn't find values for these constants at higher or lower T we have assumed these values to be correct for all T. Furthermore because Raman scattering is caused by asymmetry in the scattering molecules and this asymmetry is temperature independent, it is likely F_{K}, ρ, and ϵ are also temperature independent.

Molecule	F_k	λ	ρ	B_0 (cm^{-1})	g_J for even J	g_J for odd J
H_2	1.0378 [11][12][13]	0.2 - 20 μm	0.0221 [11]	59.3345 [14]	1 [15]	3 [15]
N_2	1.034	see[9],[16]	0.02106 / 0.0303[11]	1.98973	6 [10]	3 [10]
CO_2	1.1364	see [9]	0.0747	0.39020 [10]	1 [10]	1 [10]

Table 1: Values for the constants needed to calculated the rotational Raman spectra of various molecules. Values for F_k at $\lambda =$ nm.

2.2.3 The Raman spectrum

As can be seen in equation 6 the strength of the exact shape of a Raman will depend on he temperature of the scattering gas. In practice this means that the quantum number J for which the contribution to the Raman spectrum must be taken into account in a model will increase. The highest J that must be taken into account further decreases with increasing B_0. Figure 1 shows the positions of the lines.

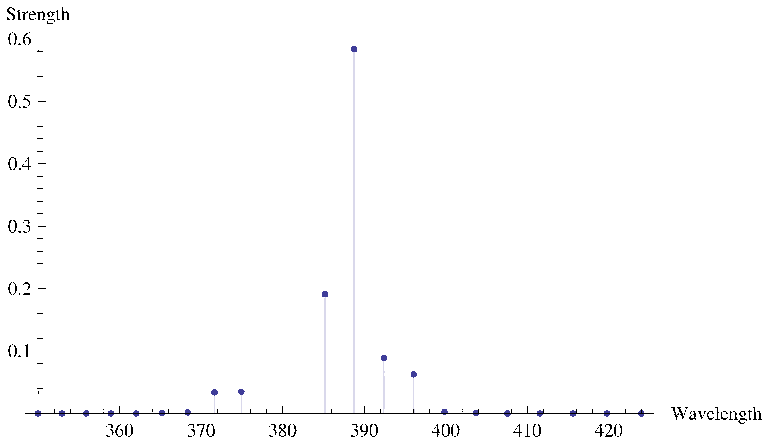

Figure 1: The Raman spectrum of an H_2 atmosphere for 380nm at a temperature of 300K. The positions of the lines indicate what wavelengths incoming photons at 380nm can be scattered to.

3 Geometries in the Problem.

3.1 Definitions of involved angles

Because we generally get the spectrum of a planet from the entire planet, not the individual points on the planet, we need to integrate the local spectra over the entire planet. We also need to keep in mind the fact that we see less of the same surface area if this surface area is more to the side of the planet, as seen from the Earth. Further more the local solar (or stellar) zenith angle, θ_0 changes with position on the sphere, as well as the reflection angle, θ and the difference in azimuth angle between incoming and reflected beam, $\phi - \phi_0$. We further use the following angles (see also figures 2 and 3):

- α, the angle between the star S, planet (P in fig 2) and the Earth E. This is the orbital phase angle.
- η, the angle between a point Q, the origin O and the northpole (P in fig. 3)
- ζ, the angle between the projection of OQ on the xy-plane and the line OE, in the direction of the Earth.

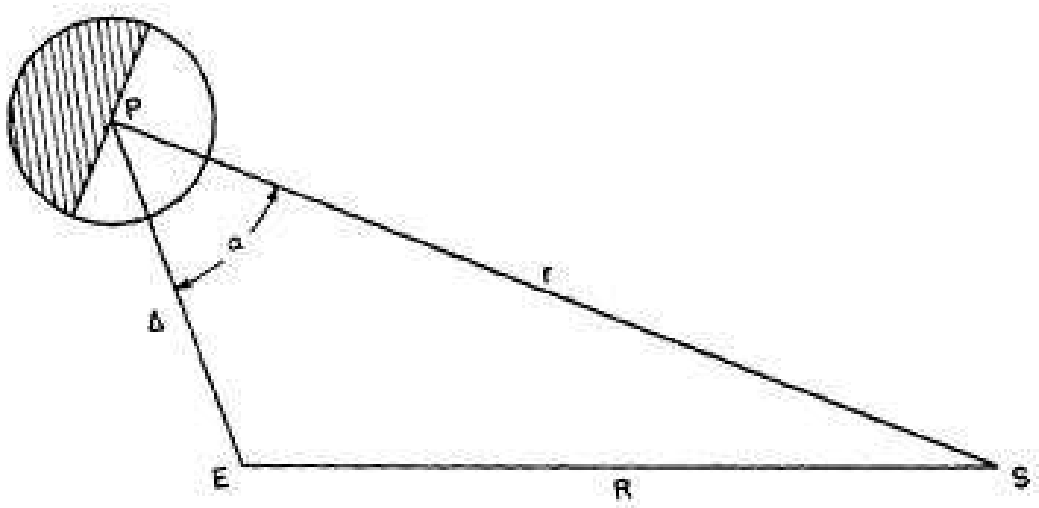

Figure 2: Topdown view of the star-planet-Earth involved in the problem. Source Horak (1950) [17]

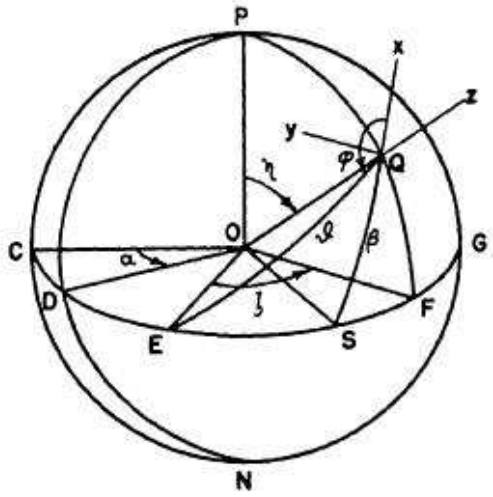

Figure 3: Part of the geometries involved in the problem, shown on a planet. Source Horak (1950) [17]

In all these cases we take the xy-plane to be the plane containing the star, the planet and the Earth. To determine (the cosines) of the involved angles I write the normal Carthesian coordinates in the appropriate angles. The angalur location of the position of a point Q then becomes

$$\vec{Q} = \begin{pmatrix} \sin\eta\cos\zeta \\ \sin\eta\sin\zeta \\ \cos\eta \end{pmatrix} \tag{7}$$

The vector for the direction of the incoming light is:

$$\vec{F}_{\text{in}} = \begin{pmatrix} \cos\alpha \\ \sin\alpha \\ 0 \end{pmatrix} \tag{8}$$

The direcion of the reflected light is:

$$\vec{F}_{\text{ref}} = \begin{pmatrix} 1 \\ 0 \\ 0 \end{pmatrix} \tag{9}$$

3.2 Calculating θ_0, θ and $\phi - \phi_0$

3.2.1 Planetary orbit without inclination

The solar/stellar zenith angle, θ_0 is the angle between incoming light and the local vertical. In general, for two vectors, $\vec{a}$ and $\vec{b}$ with an angle γ between them we have:

$$\cos\gamma = \frac{\vec{a}\cdot\vec{b}}{|\vec{a}||\vec{b}|} \tag{10}$$

$$\sin\gamma = \frac{|\vec{a}\times\vec{b}|}{|\vec{a}||\vec{b}|} \tag{11}$$

And further for any four vectors a, b, c and d we have:

$$(\vec{a}\times\vec{b})\cdot(\vec{c}\times\vec{d}) = (\vec{a}\cdot\vec{c})(\vec{b}\cdot\vec{d}) - (\vec{a}\cdot\vec{d})(\vec{b}\cdot\vec{c}) \tag{12}$$

In the is case the vector are all have norm unity, so equation 10 reduces to $\cos\theta = \vec{a}\cdot\vec{b}$. Using this θ and θ_0 become:

$$\cos\theta_0 = \vec{F}_{\text{in}}\cdot\vec{Q} = \begin{pmatrix} \cos\alpha \\ \sin\alpha \\ 0 \end{pmatrix} \cdot \begin{pmatrix} \sin\eta\cos\zeta \\ \sin\eta\sin\zeta \\ \cos\eta \end{pmatrix} = \sin\eta\cos\zeta\cos\alpha + \sin\eta\sin\zeta\sin\alpha = \sin\eta\cos(\zeta-\alpha) \tag{13}$$

$$\cos\theta = \vec{F}_{\text{ref}}\cdot\vec{Q} = \begin{pmatrix} 1 \\ 0 \\ 0 \end{pmatrix} \cdot \begin{pmatrix} \sin\eta\cos\zeta \\ \sin\eta\sin\zeta \\ \cos\eta \end{pmatrix} = \sin\eta\cos\zeta \tag{14}$$

Further the definitions $\cos\theta = \mu$ and $\cos\theta_0 = \mu_0$ are often used.

The angle $\phi - \phi_0$ is the angle between the plane containing $\vec{F}_{\text{in}}$ and $\vec{Q}$ (plane 1, normal vector $\hat{n}_1$) and the plane containing $\vec{F}_{\text{ref}}$ and $\vec{Q}$ (plane 2, normal vector $\hat{n}_2$). The angle between two planes, is the angle between their normal vectors, $\hat{n}_1$ and $\hat{n}_2$. We can calculate $\hat{n}_1$ and $\hat{n}_2$ using:

$$\hat{n}_1 = \frac{\vec{F}_{\text{in}}\times\vec{Q}}{|\vec{F}_{\text{in}}\times\vec{Q}|} \tag{15}$$

$$\hat{n}_2 = \frac{\vec{Q}\times\vec{F}_{\text{ref}}}{|\vec{Q}\times\vec{F}_{\text{ref}}|} \tag{16}$$

The angle $\phi - \phi_0$ then becomes:

$$\cos(\phi-\phi_0) = \hat{n}_1\cdot\hat{n}_2 = \frac{(\vec{F}_{\text{in}}\times\vec{Q})\cdot(\vec{Q}\times\vec{F}_{\text{ref}})}{|\vec{F}_{\text{in}}\times\vec{Q}||\vec{Q}\times\vec{F}_{\text{ref}}|} \tag{17}$$

Using equation 12 this becomes:

$$\cos(\phi - \phi_0) = \frac{(\vec{F}_{\text{in}} \cdot \vec{Q})(\vec{Q} \cdot \vec{F}_{\text{ref}}) - (\vec{F}_{\text{in}} \cdot \vec{F}_{\text{ref}})(\vec{Q} \cdot \vec{Q})}{|\vec{F}_{\text{in}} \times \vec{Q}||\vec{Q} \times \vec{F}_{\text{ref}}|} \tag{18}$$

Finally using $\vec{Q} \cdot \vec{Q} = 1$ and $\vec{F}_{\text{in}} \cdot \vec{F}_{\text{ref}} = \cos\alpha$ we find the following expression for $\cos(\phi - \phi_0)$:

$$\cos(\phi - \phi_0) = \frac{\cos\theta_0 \cos\theta - \cos\alpha}{\sin\theta_0 \sin\theta} \tag{19}$$

This expression for $\cos(\phi - \phi_0)$ is equal to the one given by Horak (1950) [17]

3.2.2 Planetary orbit with inclinination, $\sin i \neq 1$

The aforementioned formulae for $\cos\theta_0$, $\cos\theta$ and $\cos(\phi - \phi_0)$ are only valid in the case of where the inclination of the planets orbit ,$i = 90°$. For the general case the vector $\vec{F}_{\text{in}}$ becomes:

$$\vec{F}_{\text{in}} = \begin{pmatrix} \sin\alpha \cos\alpha \sin i \\ \sin^2\alpha \sin i \\ \cos\alpha \cos i \end{pmatrix} \tag{20}$$

As a result of this the expressions for $\cos\theta_0$ and $\cos(\phi - \phi_0)$ in equations 13 and 19 will change, while the expression for $\cos\theta$ in equation 14 will remain unchanged. This is because $\vec{F}_{\text{in}}$ is not used in deriving an expression for $\cos\theta$. The new expressions are:

$$\cos\theta_0 = \sin\eta \sin\alpha \sin i \cos(\zeta - \alpha) + \cos\eta \cos\alpha \cos i \tag{21}$$

$$\cos(\phi - \phi_0) = \frac{\cos\theta_0 \cos\theta - \sin\alpha \cos\alpha \sin i}{\sin\theta_0 \sin\theta} \tag{22}$$

These equations are equivalent to changing the angle α in section 3.2.1 to $\cos\alpha_{\text{used}} = \cos\alpha \sin i$.

3.2.3 Calculating β

To express β, as introduced in section 2, in terms of the θ, θ_0, $\phi - \phi_0$, α and i, one has to use spherical geometry. Figure 4 shows the angles needed to calculate β. Following the definitions used by Weisstein [18]

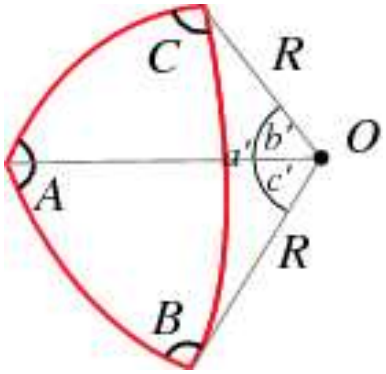

Figure 4: The angles involved in the determination of an expression of β in terms of θ, θ_0, $\phi - \phi_0$, α and i. Source: http://mathworld.wolfram.com/SphericalTrigonometry.html [18]

we have:

$$\vec{a} = \overrightarrow{OA} = \vec{Q}$$
$$\vec{b} = \overrightarrow{OB} = \vec{F_{\text{ref}}}$$
$$\vec{c} = \overrightarrow{OC} = \vec{F_{\text{in}}}$$
$$a' = \angle BOC = \arccos(\sin\alpha \cos\alpha \sin i)$$

$$b' = \angle COA = \theta_0$$
$$c' = \angle AOB = \theta$$
$$A = \angle BAC = \phi - \phi_0$$
$$B = \angle ABC = \beta$$
$$C = \angle BCA$$

The angles A and C are listed for completeness, they are not used in the further determination of an expression for β. The expressions in [18] also depend on the radius, R of the sphere for which the calculations are done, here we have used $R = 1$. Using equation 11 from Weisstein [18]:

$$\cos b' = \cos a' \cos c' + \sin c' \sin a' \cos B \tag{23}$$

Solving this for B and substituting with the angels θ, θ_0, $\phi - \phi_0$, α and i we find:

$$\beta = \arccos\left(\frac{\cos\theta_0 - \cos\theta \sin\alpha \cos\alpha \sin i}{\sin\theta \sin(\arccos(\sin\alpha \cos\alpha \sin i)}\right) \tag{24}$$

4 Integration over a planet's surface

Because the code only gives the polarized spectrum at a certain point on the planet's surface, it is necessary to integrate the calculated specra across the entire visible disk. The intensity vector($\vec{I}_{\text{tot}}$) of the light reflected in the direction of an observer is (Stam et al. (2006) [19])

$$\vec{I}_{\text{tot}} = \int_{\text{visible disk}} \mu \vec{I}(\mu, \mu_0, \phi - \phi_0) \text{d}O \tag{25}$$

Where $\vec{I}(\mu, \mu_0, \phi - \phi_0)$ is the intensity of the light reflected in the direction of the observer a by point on the surface of the planet and $dO = d\mu d\kappa = \sin(\eta) d\eta d\zeta$. In μ, κ coordinate system μ changes radially and κ is an angle spanning an angle of 2π Because it is easy to make a grid on the computer in Euclidean coordinates (x, y) it is convenient to rewrite equation 25 to the (x, y) coordinate system. In this case equation 25 becomes:

$$\vec{I}_{\text{tot}} = \int_{\text{visible disk}} \vec{I}(x, y) \text{d}x\text{d}y \tag{26}$$

Where $\vec{I}(x, y)$ is the calulated polarized spectrum at a point (x, y) on the disk.

4.1 Proof

Consider the disk of the planet and place a grid over it with $(x, y) = (0, 0)$ at the center of the disk. Then the angles η and ζ at position (x, y) become:

$$\eta = \arccos(y) \tag{27}$$

$$\zeta = \arcsin\left(\frac{x}{\sqrt{1 - y^2}}\right) \tag{28}$$

Then the integral of any function $f(\eta, \zeta)$ over the visible disk is:

$$f_{\text{tot}} = \int \mu(\eta, \zeta) f(\eta, \zeta) \mu(\eta, \zeta) \text{d}\eta \text{d}\zeta \tag{29}$$

Where the term $\mu(\eta, \zeta)$ is included to account for the fact that observed size of a surface area on a sphere is smaller than its actual area. Equation 29 equals

$$f_{\text{tot}} = \int f(x, y) \mu(x, y) J \text{d}x\text{d}y \tag{30}$$

Where J is the determinant of the Jacobi matrix, in this case equaling:

$$J = \begin{pmatrix} \frac{\partial \eta}{\partial x} & \frac{\partial \eta}{\partial y} \\ \frac{\partial \zeta}{\partial x} & \frac{\partial \zeta}{\partial y} \end{pmatrix} = \begin{pmatrix} 0 & -\frac{1}{\sqrt{1-y^2}} \\ \frac{1}{\sqrt{1-y^2}\sqrt{1-\frac{x^2}{1-y^2}}} & \frac{xy}{\sqrt{1-y^2}^{3/2}\sqrt{1-\frac{x^2}{1-y^2}}} \end{pmatrix} \tag{31}$$

And the determinant of J, det(J) is then:

$$\det(J) = \frac{1}{(1 - y^2)\sqrt{1 - \frac{x^2}{1-y^2}}} \tag{32}$$

If we now use $\mu = \sin^2(\eta)\cos(\zeta)$ (equation 10) the it is easy to show that

$$\sin^2(\eta)\cos(\zeta)\det(J) = 1 \tag{33}$$

4.2 Numerical integration

In the numerical integration one also has to take a factor of μ_0 into account. The total numerical integral over all intensities in an $N \times N$ grid now becomes,

$$\pi F = \frac{\pi}{4} \sum_{i,j} \mu_0 I(x_i, y_j) \text{d}O \tag{34}$$

Where x_i and y_j are in the take to be in the center of the cell, $I(x_i, y_j)$ is the calculated intensity at postition (x_i, y_j), the term $\frac{\pi}{4}$ is a normalization factor, see also equation (13) in Stam et al. (2006) [19].

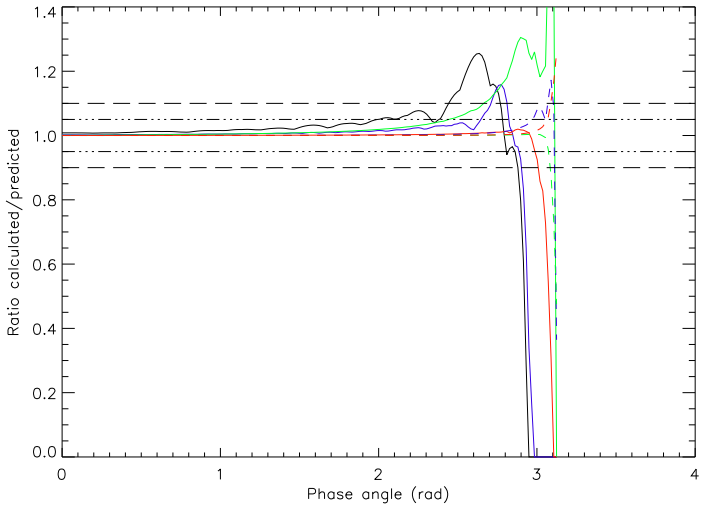

Figure 5: Ratio between the numerical calculated Lambertian flux and analytically predicted flux, for several $N \times N$ grids. Black: $N = 10$, blue: $N = 20$, green: $N = 50$, red: $N = 100$, dashed blue: $N = 200$, dashed green: $N = 500$, dashed red: $N = 1000$

4.3 Testing the numerical integration

A way of testing the integration algorithm is the to see if the numerical integration gives the right flux for a Lambertian reflector. Stam et al. (2006) [19] (following Van de Hulst (1980) [20]) give an analytical expression for a Lambertian reflector of radius 1:

$$\pi F = \frac{8}{3\pi}(\sin\Theta - \Theta\sin\Theta) \tag{35}$$

Where $\Theta = 180^\circ - \alpha$. Figure 5 gives an overview of the ratio between the numerically calculated flux and the analytical prediction. From this figure it can be seen that even a 10×10 grid remains accurate to within 10% of the predicted value upto an angle of approximately 2.4 rad. It must be noted that only the total flux can be tested using a Lambertian reflector. So it is possible that a larger grid is needed to accurately determine the total degree of polarization of a planet. However we hope (and assume) total polarization has an accuracy similar to the accuracy of of the flux using the same grid.

5 Parameters Dependence of Reflected Spectra

5.1 Different molecules.

The first thing we tested is the effect on the polarized spectrum from using different molecules. The molecules tested were N_2 and H_2. These molecules were chosen because the atmosphere of Titan is over 90% N_2 and because the most abundant molecule in the atmosphere of a Hot-Jupiter is H_2. To get an idea of the effect of using different molecules I calculated the polarized spectrum for several θ_0 on the eqautor of a sphere with $\alpha = 90°$. The polarized spectra were calculated between 380 and 400 nm. Difference between the polarized spectrum due to Raman scattering on H_2 and N_2 for different angles can be seen in figures 31 to 34 in Appendix C and figure 6.

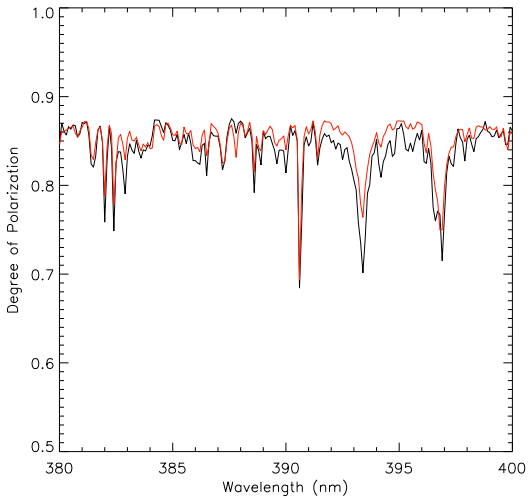

Figure 6: The calculated degree of polarization of H_2 (black) and N_2 (red) between 380nm and 400nm. $\theta = 0.1°, \theta_0 = 89.9°$.

5.2 Temperature dependence

The second test was to see to what extend the calculated spectra are sensitive to the temperature in the scattering layers of a planetary atmosphere. Stam et al. (2002) [5] already noted that the for Raman scattering in the Earth's atmosphere the exact temperature was of little importance. Figure 7 the dependence between temperature and absolute linedepth in degree of polarization. Where the absolute linedepth is defined as $P(\lambda)_{\text{continuum}} - P(\lambda)_{\text{line}}$

As can be seen in figure 7 the atmospheric temperature has only a small effect on the absolute polarized linedepth. This is consistent with the findings from Stam et al. (2002) [5] for the Earth's atmosphere.

5.3 Optical thickness dependence

The third tested parameter is the scattering optical depth of the scattering molecules (b^m_{sca}). The optical depth seems to have no effect on the final absolute linedepth in degree of polarization for a wide range of optical depths. This can be seen in figure 8. As a result a fixed value for the optical depth, $b^m_{sca} = 5$.

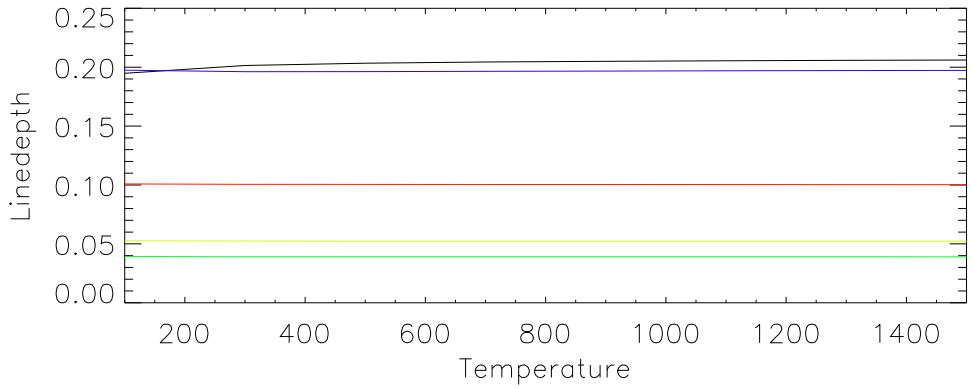

Figure 7: The temperature dependence of absolute polarized linedepth for several Fraunhofer lines. The input spectrum is that of the star τ Boo, the planetary atmosphere is 90% H_2 and 10% He. The spectra where calculated for a point on the planet with $\theta = 45°$, $\theta_0 = 45°$ and $\phi - \phi_0 = 1°$. Blue: Ca-K (393.37 nm), black: Ca-H (396.85 nm), green: Na-D (589.59 nm), yellow: Na-D (589.00 nm), red: H-α. Temperature is in K.

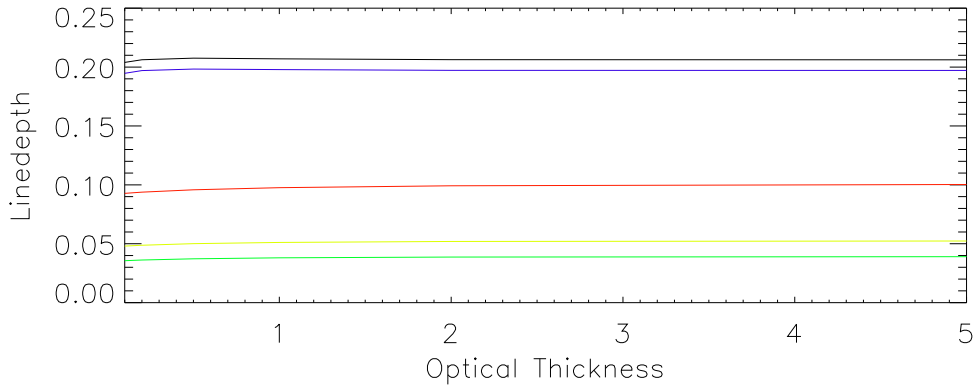

Figure 8: The optical thickness dependence of absolute polarized linedepth for a temperature of 1300K. θ, θ_0 and $\phi - \phi_0$ are the same as in figure 7. Blue: Ca-K (393.37 nm), black: Ca-H (396.85 nm), green: Na-D (589.59 nm), yellow: Na-D (589.00 nm), red: H-α.

6 Angle Dependence of Reflected Spectra

In order to determine for how many points on the surface of a planet we need to calculate the reflected spectrum, it is important to know how the reflected spectrum changes as a function of θ, θ_0 and/or $\phi - \phi_0$ and whether these changes are significant. The first test was for a the case of N_2 and H_2 atmospheres representative of Titan, former, or a gas giant, latter, with $\alpha = 90°$ on the equator of the planet. The results for 4 different locations near the equator can be seen in figures 9 and 10. Differences between N_2 and H_2 atmospheres for those same locations can be found in the appendix (figures 31, 32, 33 and 34).

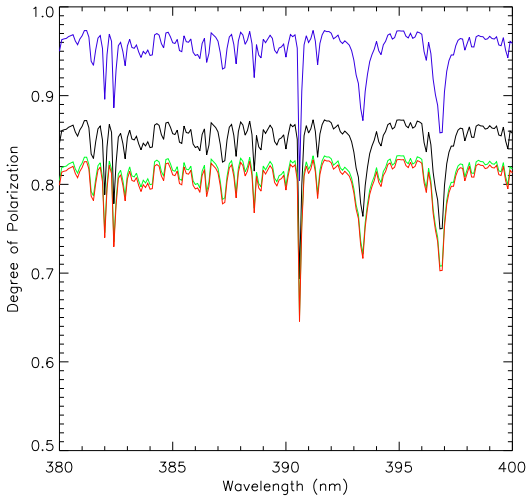

Figure 9: The calculated polarization spectra for N_2 for several combinations of (θ_0, θ). (θ_0,θ): Black ($89.9°$,$0.1°$), green ($36.87°$,$53.13°$), red ($17.46°$,$72,54°$), Blue ($0.1°$,$89.9°$)

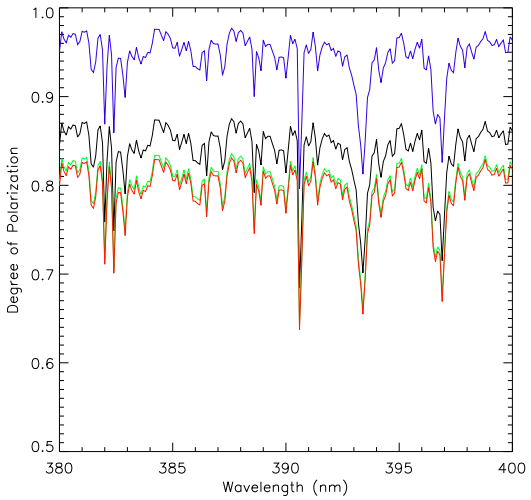

Figure 10: Same as figure 9 only for H_2.

Since the linedepth of the spectra depends on the angle, tests were performed to see if the relative linedepths might be constant for a certain phase angle. Where the relative linedepth is $\frac{P(\lambda)_{\text{continuum}} - P(\lambda)_{\text{line}}}{P(\lambda)_{\text{continuum}}}$. If this were the case computation time would be reduced significantly, since only one spectrum would have to be calculated across the entire wavelength range and for other points on the planet only a small wavelength interval would be needed. Unfortunately the relative linedepth turned out not to be constant over the planets surface for a single value of α and therefore the calculation had to be done for each point in a certain grid.

7 Simulations

In order to see the change in the total degree of polarization of planet and star, we made models of the total polarization at several points of a planets orbit. We chose τ Boo-b as model planet because we have HARPS observations in linear polarization of that system made in may 2011. The important parameters for the τ Boo system can be found in Table 2. The models are for $0° \leq \alpha \leq 180°$ in intervals of $30°$. The HARPS input spectrum can be seen in figure 11.

T_{eff}	6360K
P_{orbit}	3.12 d
a	0.0489AU
$M_{\text{p}} \sin i$	$4.28 M_{\text{Jup}}$
R_{p}	$1.2 R_{\text{Jup}}$
i	$45°$
$v_{\text{max,LOS}}$	110km s^{-1}

Table 2: The parameters of the τ Boo system most important for the purposes of this work. i and $v_{\text{max,LOS}}$ from Snellen (private communication), other parameters from Leigh et al. (2003) [21]

The code as adapted from Stam et al. (2002) [5] was used to calculate the polarized spectrum on a grid placed over the planet. Next equation 2 was used to transform the Stokes' parameters, which were calculated in a local frame of reference based on the direction of the local zenith, to a planetary frame of referrence. After this the results for all points on the grid were added up, i.e. numerically integrated and the degree of polarization of the entire planet determined. The degree of polarization gotten this way is not yet correct. Although the absolute linedepth, i.e. $\Delta P(\lambda) = P_{\text{continuum}}(\lambda) - P_{\text{line}}(\lambda)$, is correct, the value for the continuum degree of polarization, $P_{\text{continuum}}$ is not. We used a code by Stam calculate the correct continuum degree of polarization for the entire planet and corrected the degree of polarization of the planet accordingly.

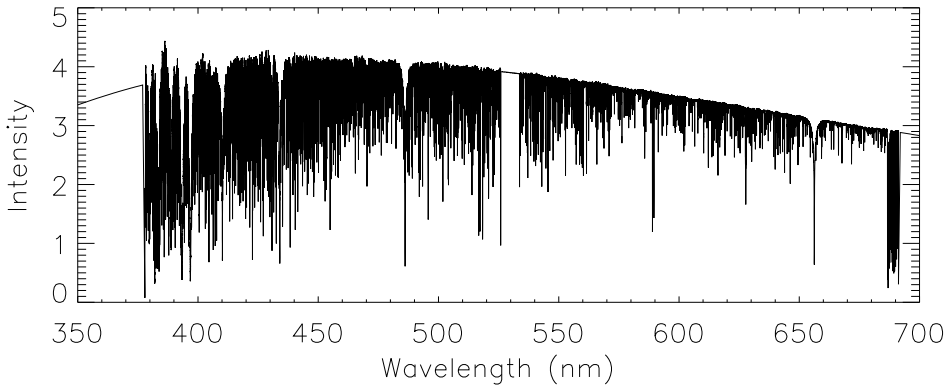

Figure 11: The HARPS intensity input spectrum. The intensity is in arbitrary units, because the original spectrum had been normalized. To get the used spectrum, the normalized spectrum was multplied by a Planck function with $T = 6360K$.

Figure 12 on page 17 shows the change in the degree of polarization integrated over the visible part of the planet as a funtion of α. Depending on the orbital phase the total degree of polarization changes by roughly a factor of 2.5, independent of wavelength. We see the greatest degree of polarization for $\alpha = 90°$, i.e. when the planet is next to the star as seen from the earth. This is as expected since polarization effects are greatest for light scattered at an angle of $90°$ which is the case for $\alpha = 90°$. However since the model planet is located at a small distance from its parent star it is unlikely to be spatially resolved from the star and therefore it is necessary to include the starlight in the simulations for the final degree of polarization. The models for just a planet might still be used in case it is possible to spattially resolve the planet and most of the starlight can be blocked using a coronagraph.
In order to include the starlight in the final polarization spectrum the planetary will first have to be Doppler

shifted, since at each point in its orbit the planet has a velocity along the line of sight. Doppler shift is taken into account by shifting all wavelength by a factor $\frac{c+v}{c}$ where $v = v_{\text{orbit}} \sin\alpha \sin i = v_{\text{max,LOS}} \sin i$. The flux and polarization are then interpolated to the original wavelengths and the flux of the star is added. Mathematically this can be written as:

$$P_{\text{total}}(\lambda) = \frac{I_{\text{planet}}(\lambda) P_{\text{planet}}(\lambda)}{I_{\text{star}}(\lambda) + I_{\text{planet}}(\lambda)} \tag{36}$$

Where I_{planet} is the Doppler shifted intensity of the light reflected of the planet, P_{planet} is the corresponding degree of polarization and I_{star} is the intensity of the star. The resulting polarization can be seen in figures 13 and 14. Whereas it was still possible to see individual lines in the spectrum of only the planet this is no longer the case if we look at the polarization of star and planet unless there is no Doppler shift which is the case for $\alpha = 0° = 360°$ and $\alpha = 180°$ at which point $\sin\alpha = 0$ and therefore the planet does not move along the line of sight. There is a small region around 530nm that does not show a chaotic polarization pattern in figures 13 and 14 however this is simply because these wavelength are not present in the original HARPS input spectrum and have been approximated with a Planck function with the temperature of τ Boötis as given in table 2.
Figure 15 shows a comparison of the polarized line structure of just the planet and of the planet and star for several of the Fraunhofer lines. Here it is clear that in fact lines can still be found when there are fewer overlapping lines in the spectrum of the star, i.e. for longer wavelength. However the lines that can be found show both an increase and a decrease in degree of polarization relative to the continuum polarization.
The reason for this somewhat chaotic behaviour of the degree of polarizations is caused by the Dopplershift. It is because generally a Doppler shifted line in the spectrum of the planet will coincide with the continuum of the star's spectrum and a line in the star's spectrum will coincide with the continuum of the planet's spectrum. Because of this the total degree of polarization will go down when the planet's spectrum has an absorbtion line and it will go up when the star's spectrum has an absorbtion line. The fact that there are many lines in the spectrum of the star and therefore in the reflected spectrum means that the cumalative of lines and continuum overlapping becomes chaotic.
The chaotic behaviour of much of the final polarization spectrum, which will be different for every value of α, will make it very hard, if not impossible, to observe the effects of raman scattering in the planetary atmosphere in cases where the planet can not be spatially resolved from its parent star.
For comparison figure 16 shows the predicted degree of polarization for a spatially unresolved planet in case its orbit has an inclination of $90°$, i.e. there is no Doppler shift because the planet moves around its star perpendicular to the line of sight. In this case many of the lines can still be seen in the polarization spectrum. However the lines that can be seen are at shorter wavelengths ($\lambda \lesssim 500$nm) whereas the lines at larger wavelength ($\lambda \gtrsim 550$nm) can no longer be seen. For these lines adding the intensities of planet and star has the effect of resulting in the same degree of polarization for the continuum and for the line, since for these lines it happens to be the case that

$$\frac{P_{\text{p,line}} I_{\text{p,line}}}{I_{\text{star}} + I_{\text{planet,line}}} = \frac{P_{\text{p,continuum}} I_{\text{p,continuum}}}{I_{\text{star}} + I_{\text{p,continuum}}}$$

. In fact even without Dopplershift it is possible for the degree of polarization of star and planet to be higher in line than the degree of polarization of continuum.

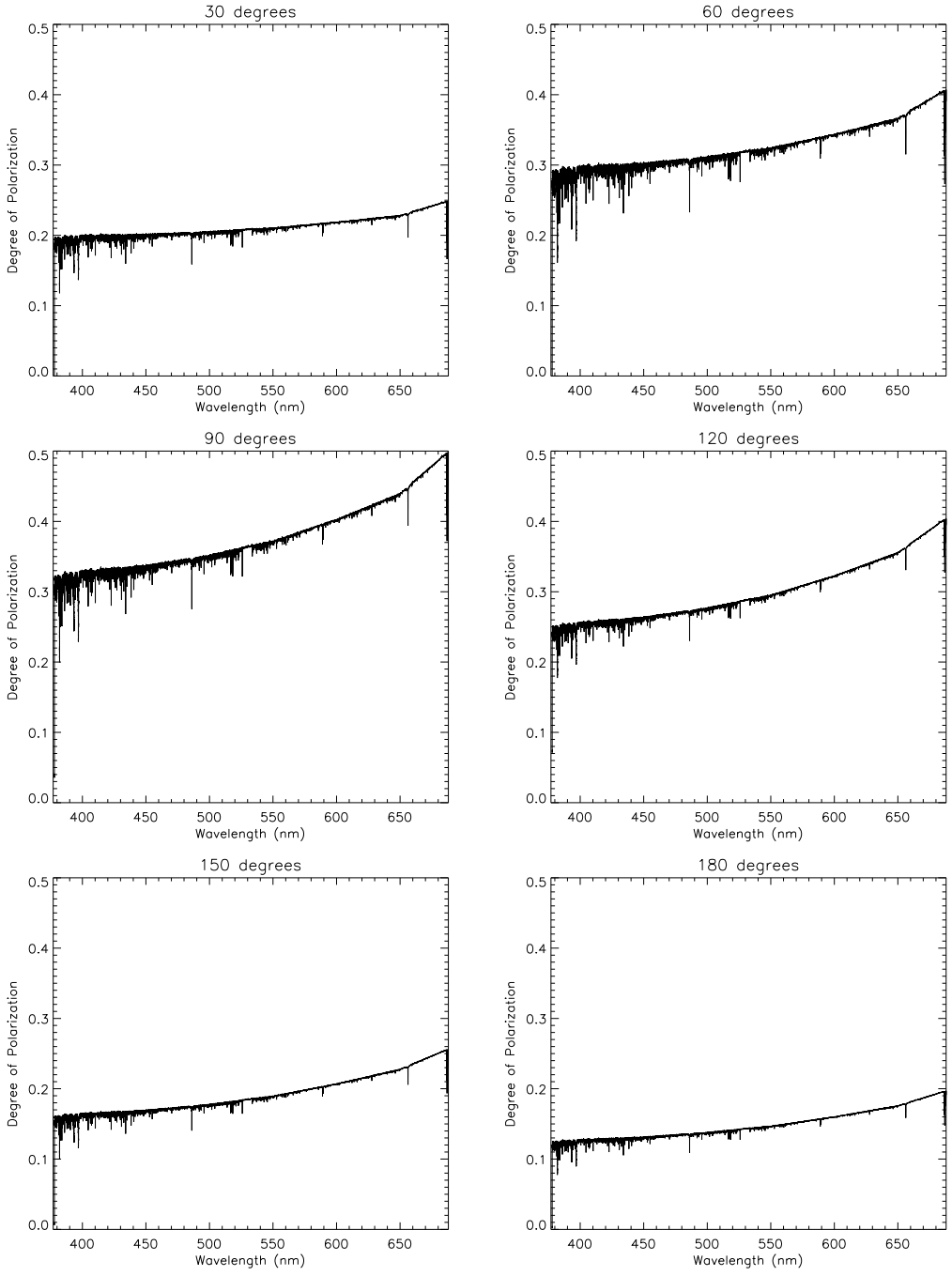

Figure 12: The degree of polarization of the light reflected of the planet at various points of its orbit. The used atmosphere is 90% H_2 and 10% He at a temperature of 1300K. No frame for $\alpha = 0°$ is included, the degree of polarization for $\alpha = 0°$ is however very similar to the degree of polarization of $\alpha = 180°$.

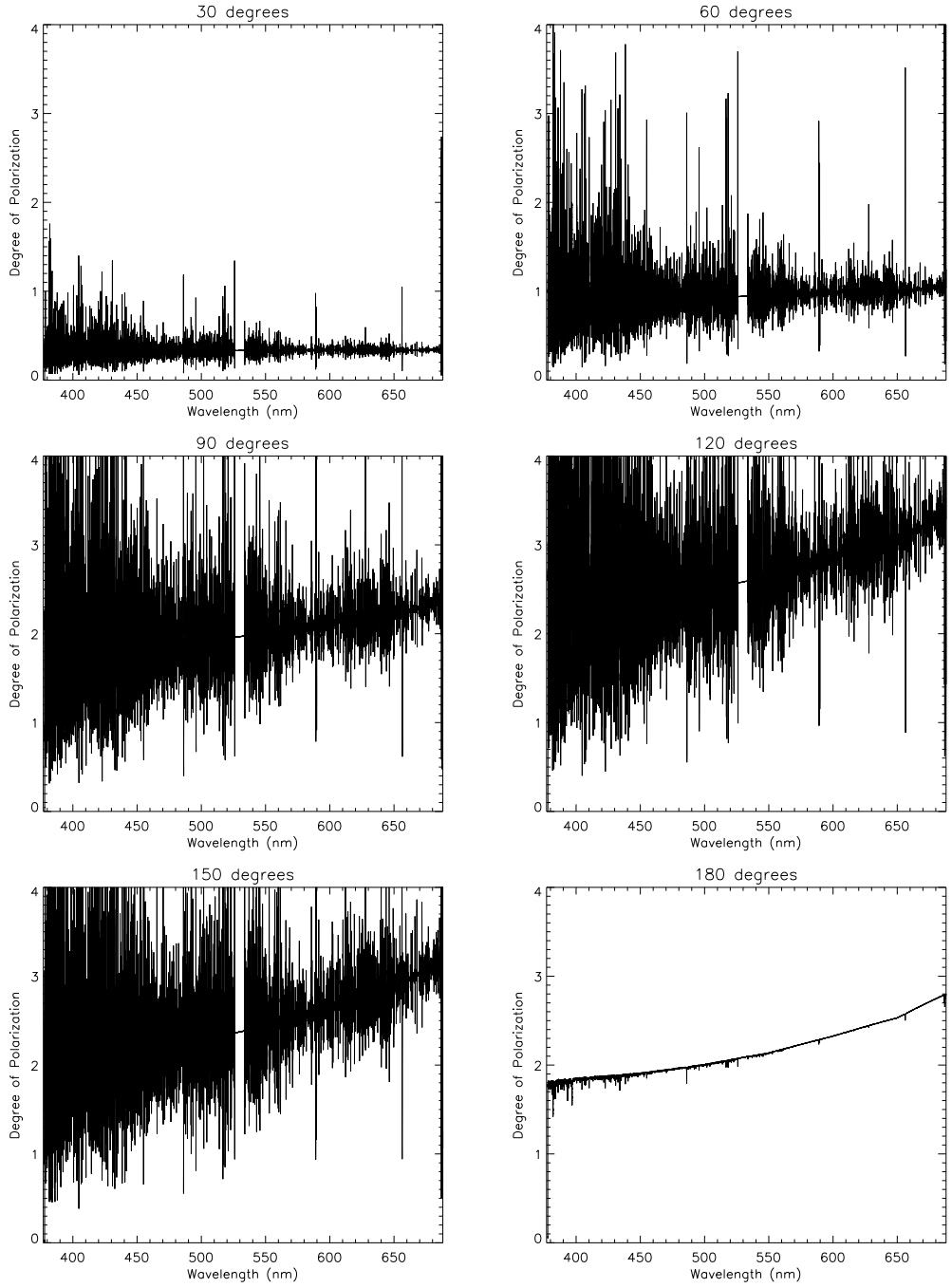

Figure 13: The degree of polarization of the light reflected of the planet and star at various points of the orbit with $30^\circ \leq \alpha \leq 180^\circ$. For comparison purposes the y-axis of all frames are to the same scale. Further all values on the y axes have been multiplied by 10^6. The planetary atmosphere is the same as in figure 12.

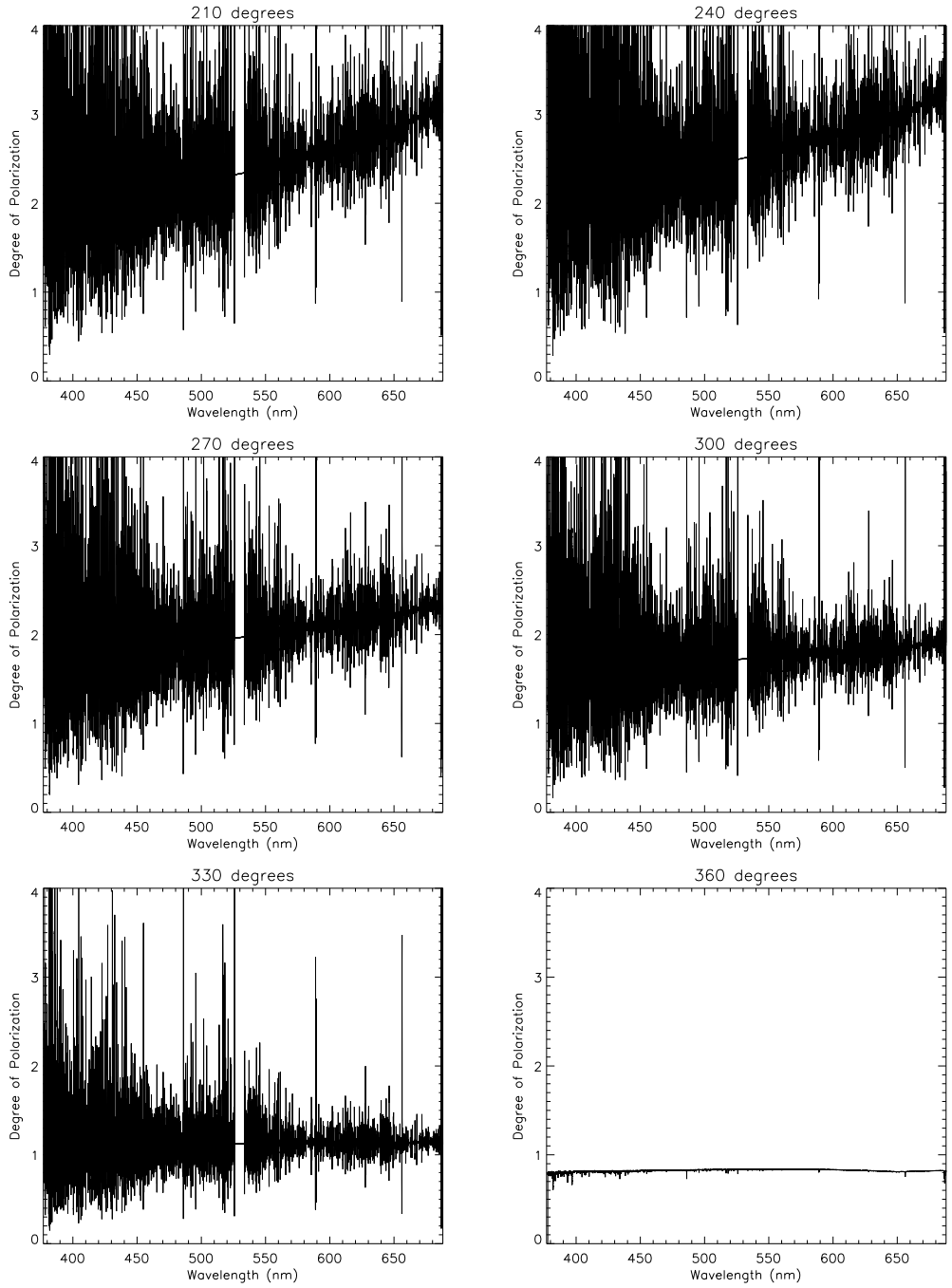

Figure 14: Same as figure 13, however in this case $210° \leq \alpha \leq 360°$. The planetary atmosphere is the same as in figure 12.

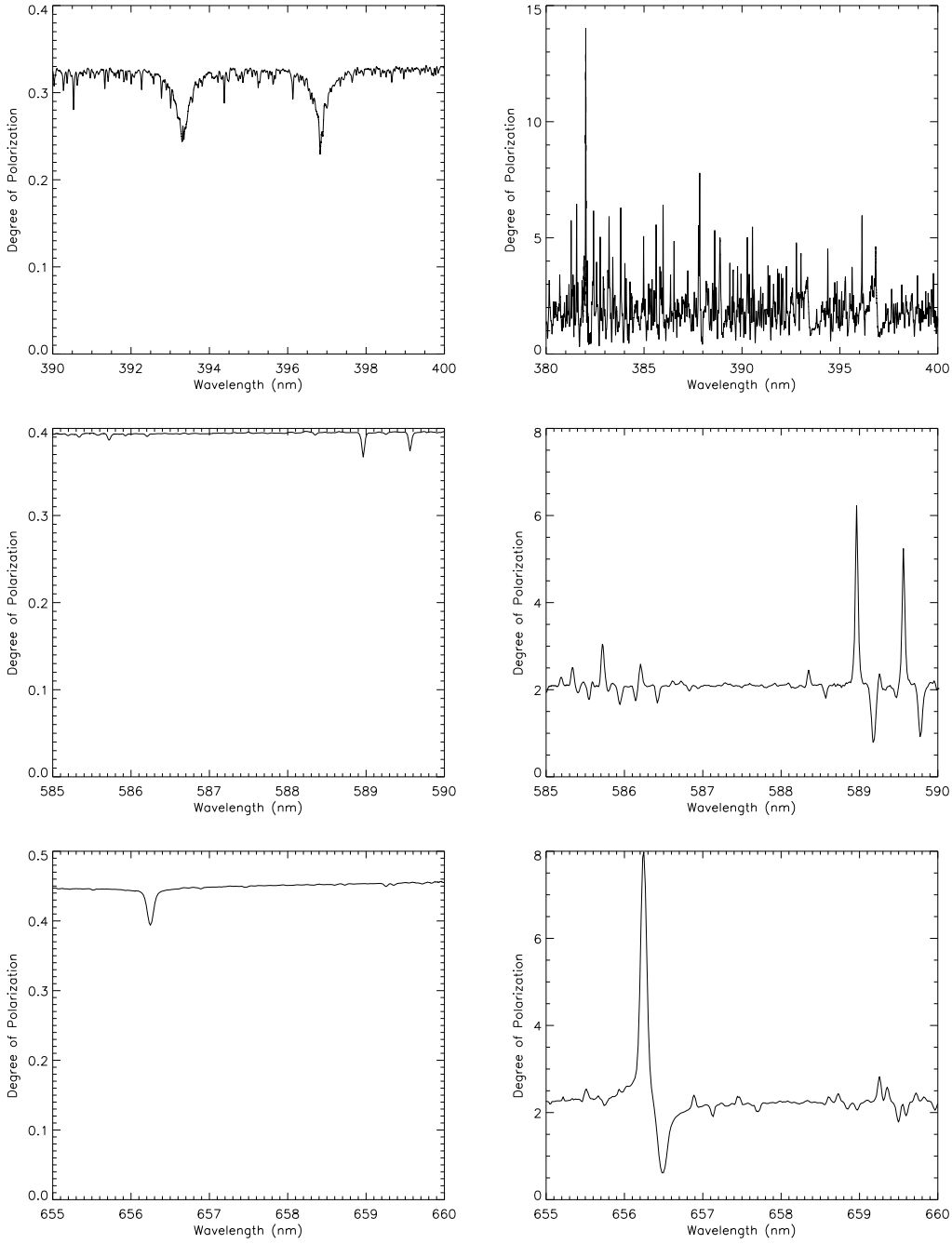

Figure 15: The degree of polarization for a wavelength region around the Ca-H/K lines for $\alpha = 90°$. Left panel: The degree of polarization of planet. Right panel: The degree of polarization of the planet and star. The values on the y-axis have been multiplied by 10^6. The planetary atmosphere is the same as in figure 12.

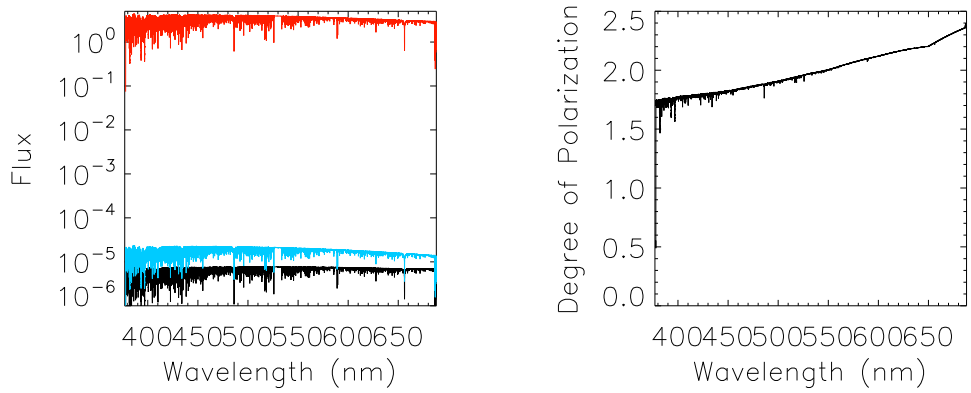

Figure 16: Left: the flux of the star (red), the planet (blue) and the polarized light (black) for a planet orbiting its star at an inclination of $90°$, orbital parameters are the same as for τ Boötis. Right: The final degree of polarization for the same planet. Values on the y-axes have been multiplied by a factor 10^6. The planetary atmosphere is the same as in figure 12.

8 Conclusions and Discussion

As seen in figures 13 and 14 the effect of adding the light of the parent star to the Doppler shifted, partially polarized light of a planet causes the final degree of polarization to become rather chaotic. That is the line structure which was visible in the original star spectrum and planet's polarization spectrum has disappeared. Because this problem is the result of Doppler shifting the planetary spectrum, the only angles for which there is no problem are those for which there is no radial velocity difference between the planet and the star. In this case $\sin\alpha = 0$ and therefore $\alpha = 0°$ or $\alpha = 180°$. For these values of α the continuum degree of polarization of star and planet will however also be smallest because then the total scattering angle is furthest from the ideal scattering angle of $90°$.
Another way of trying to observe Raman scattering in a exoplanet would be to look for a planet that is far enough from its parent star to be spattially resolved from the star. In this case a coronagraph could be used to filter out the star's light and a direct observation of the planet's (reflected) spectrum might be possible. These observations would likely have to be made close to $\alpha = 90°$ because at that point the degree of polarization is greatest and because the angular seperation between the planet and the star is greatest. For direct observations of Raman scattering in exoplanets it is possible to test the code on planets in our own solar system. Table 1 in section 2 lists the Raman scattering parameters for the main molecules in the atmospheres of Venus, the Earth and Saturn's moon Titan. Observations of the reflected Raman spectrum of the giant planets in the solar system would also be possible as test.
Except for the problems due to Doppler shift that have already mentioned, several other effects have not yet been taken into effect altough they are likely to have an effect on the final measured spectrum. The first of is these is the absence of a haze (dust) in the used models. The atmosphere of an exoplanet is unlikely to be purely H_2 and He instead there will likely be hazes or clouds of various composition in the atmosphere. These hazes are likely to decrease the absolute linedepth in the polarization spectrum, making it more difficult to observe the effect of Raman scattering in a the reflected spectrum. The code used for this work is capable of calculating the efffect of atmospheric hazes, however the main interest was to use models to find out if it is possible to see Raman scattering in exoplanets under ideal circumstances.
The other main problem is a shortcoming of the code itself, which only calculates two orders of scattering. As stated in section 7 the absolute linedepth in the polarized spectrum is correctly calculated, the degree of continuum polarization is however not calculated correctly. This implies that the calculated intensity is most likely also not correct. The code used to correct the continuum degree of polarization also give us the continuum intensity and could therefore be use to change the continuum of the calculated intensity to the right level. For this we assumed that the relative line depth of the intensity spectrum, i.e. $\frac{I_{\text{continuum}}(\lambda) - I_{\text{line}}(\lambda)}{I_{\text{continuum}}(\lambda)}$, was calculated correctly.
In conclusion based on the results shown in figures 13 and 14 it is likely difficult to observe the effects of Raman scattering in exoplanet atmospheres when the planet cannot be spatially resolved, especially for shorter wavelengths. The difficulty in observing Raman scattering in an unresolved planet are not just due to the more chaotic line structure caused by Doppler shifting the planetary spectrum. The low continuum order of polarization, on the order of 10^{-6} is already close to the minimum degree of polarization that can currently be observed.
There are however a several ways of making more accurate models for use on exoplanets that can be spatially resolved, the two most important are:

- Including more orders of scattering, to better calculated the continuum degree of polarization and final intensity.
- Including hazes in the model, to get more realistic values of the absolute linedepth in the polarized spectrum.

Including hazes be done in several ways. The easiest would be to include a planet covering haze of constant composition and optical thickness. A more accurate alternative would be to include local hazes of varying composition and optical thickness. This alternative would likely increase the time required to run the models on a computer.

A Viewing angles

The plots in this subsection show the lines on a planet's surface with equal θ and θ_0 assuming a certain α. Also indicated which points on a grid are used in calculating the final degree of polarization of the reflected light. All included points are given the same weight. Errors due to giving points the same weight regardless of whether they are near the edge of the planet can be seen in figure 5 on page 11

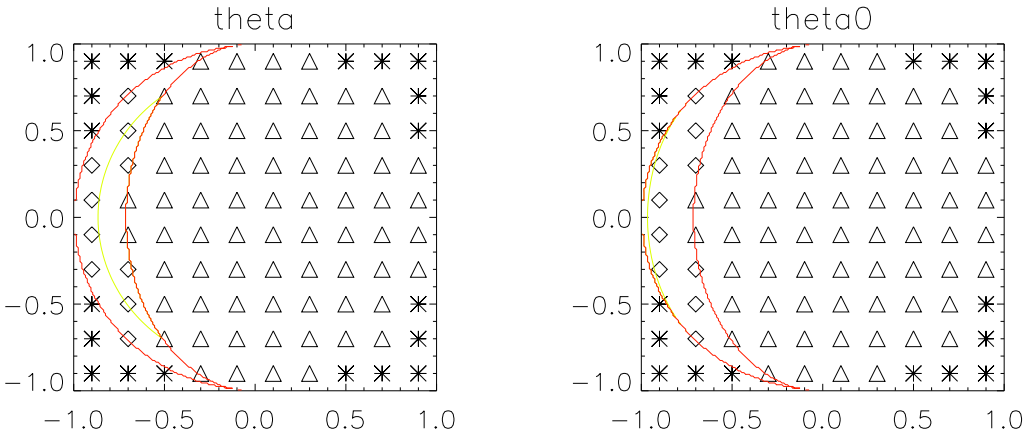

Figure 17: Contours of θ (left) and θ_0 (right) on a 10×10 grid showing which points are included in calculating the total degree of polarization of the planet for $\alpha = -135°$. A point on the planet used in the calculations is indicated by a diamond, a point on the planet which is not used, due to not being illuminated, is indicated by triangles, a point not on the planet is indicated by an asterix. The contours are blue: $\theta/\theta_0 = 30°$, yellow: $\theta/\theta_0 = 45°$, green: $\theta/\theta_0 = 60°$, red: $\theta/\theta_0 = 90°$, edge of the planet or the terminator, i.e. the line marking the boundary between where light from the star hits the planet and where this no longer happens.

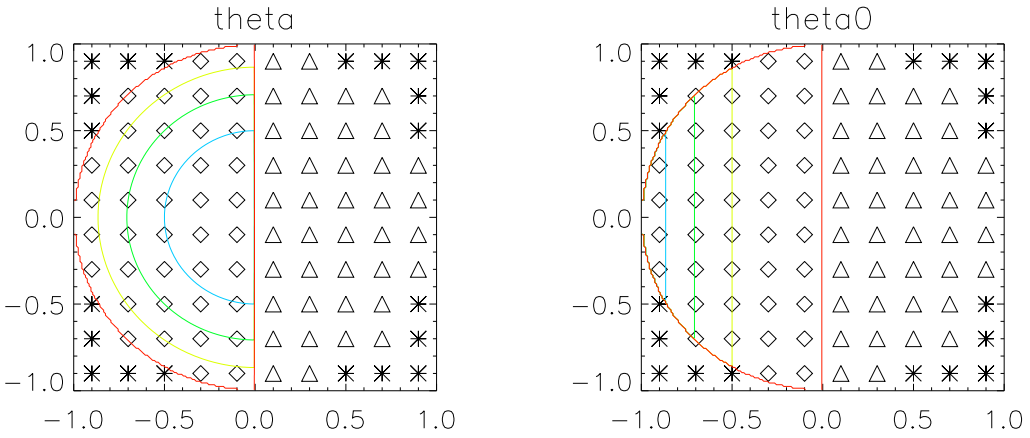

Figure 18: Same as figure 17 with $\alpha = -90°$.

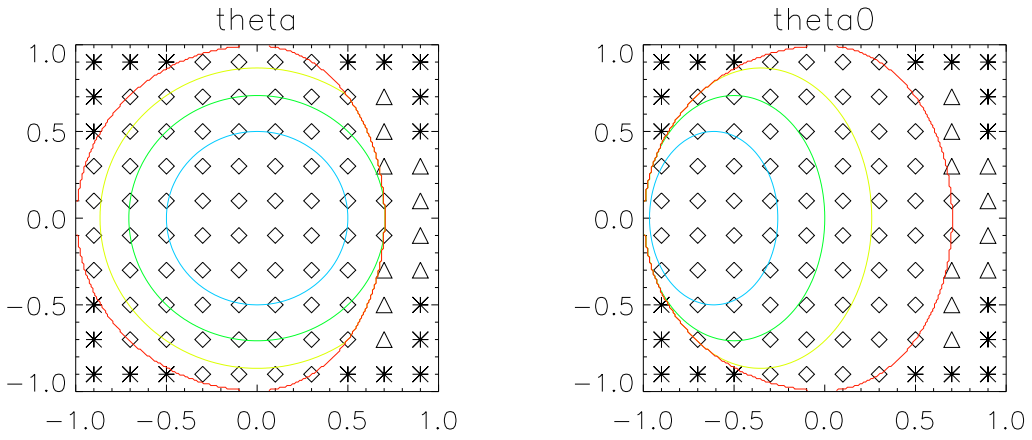

Figure 19: Same as figure 17 with $\alpha = -45°$.

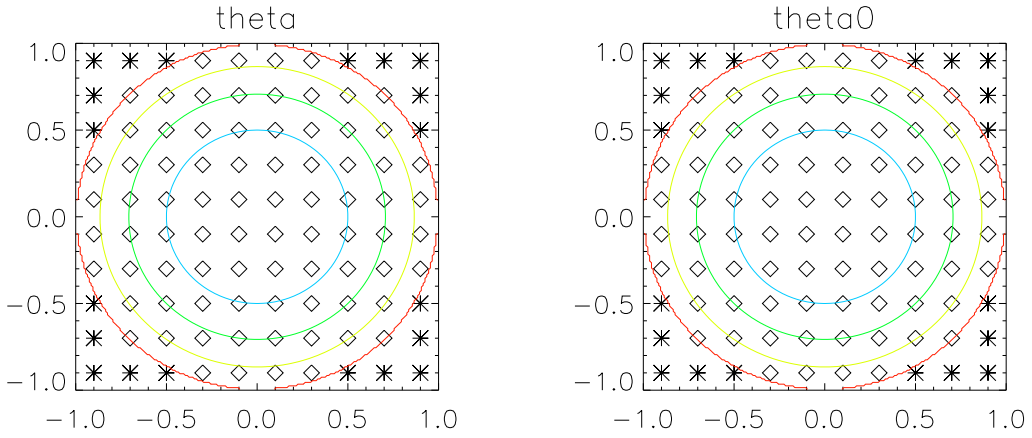

Figure 20: Same as figure 17 with $\alpha = 0°$.

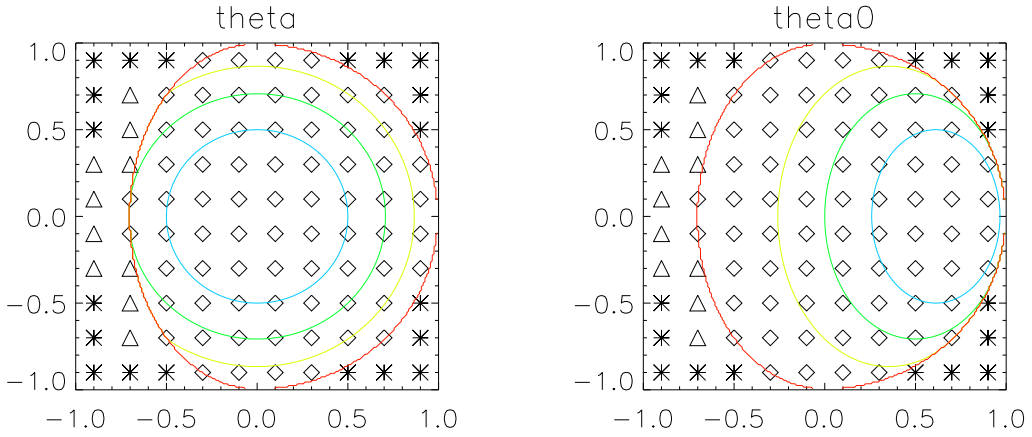

Figure 21: Same as figure 17 with $\alpha = 45°$.

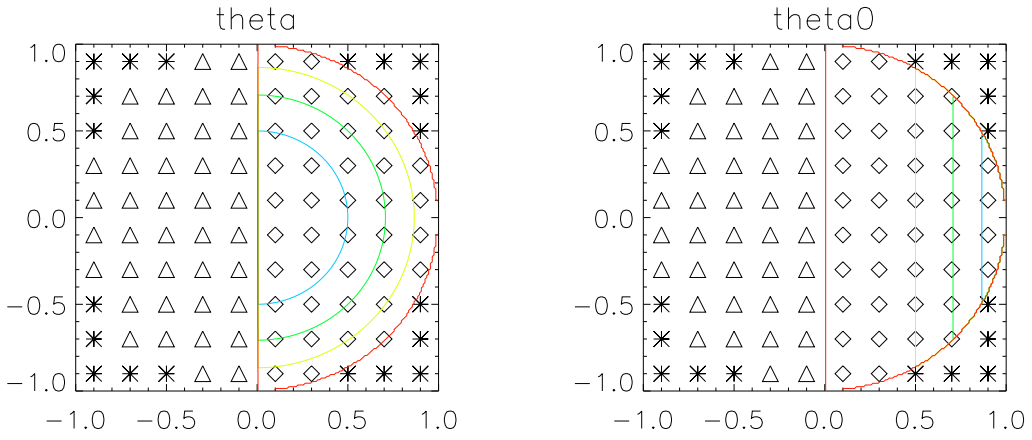

Figure 22: Same as figure 17 with $\alpha = 90°$.

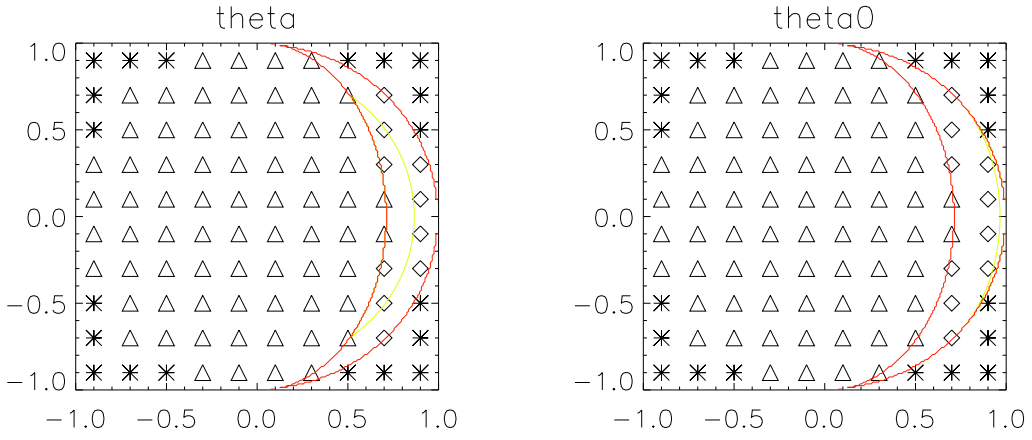

Figure 23: Same as figure 17 with $\alpha = 135°$.

B Raman Spectra

In this appendix you can find the Raman spectra of several atmospheric compositions and temperatures. The Raman spectra were calculated in terms of a wavenumber difference from the original wavelength, here these wavenumber difference have been translated to the wavelengths from which Raman scattering moves flux from a fixed wavelength, here 380nm or 680nm.

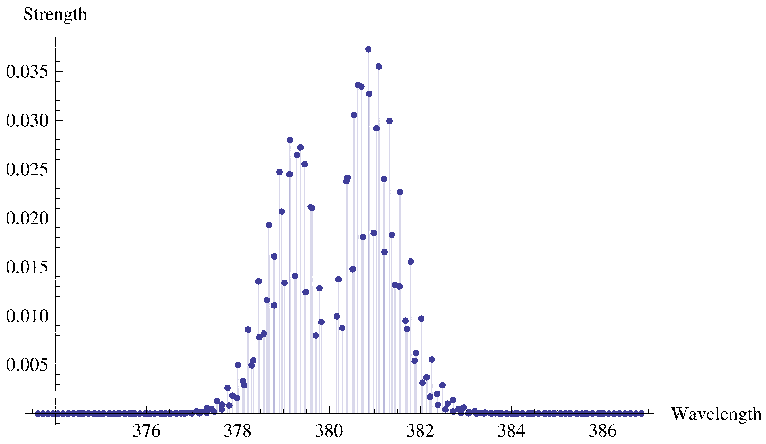

Figure 24: The Raman spectrum of the Earth's atmosphere for 380nm at a temperature of 300K.

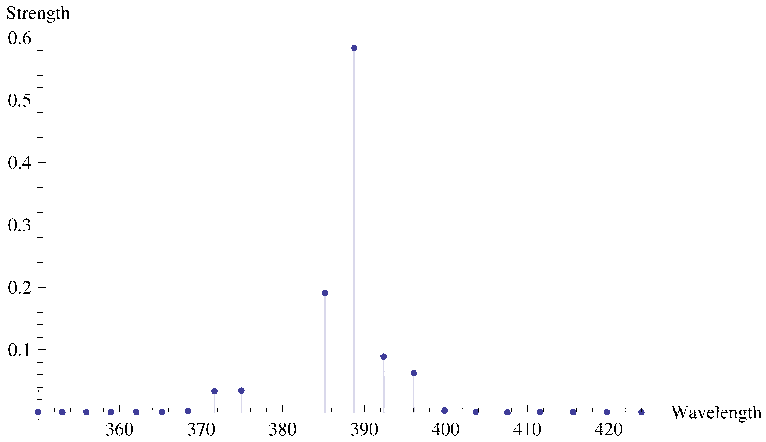

Figure 25: The Raman spectrum of H_2 for 380nm at a temperature of 300K. This figure is identical to figure 1.

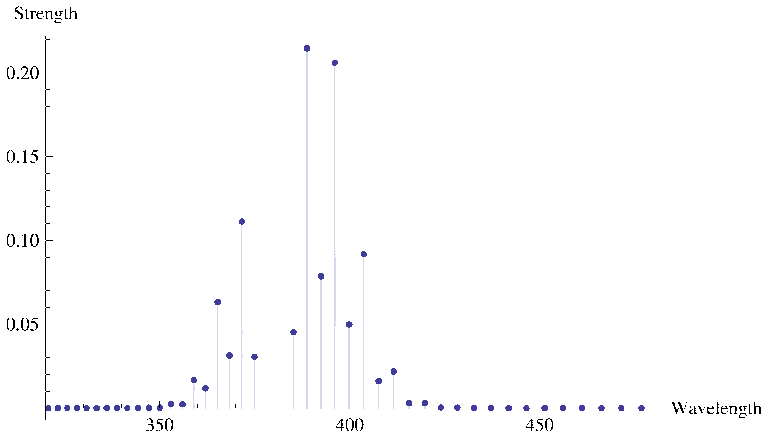

Figure 26: The Raman spectrum of H_2 for 380nm at a temperature of 1300K.

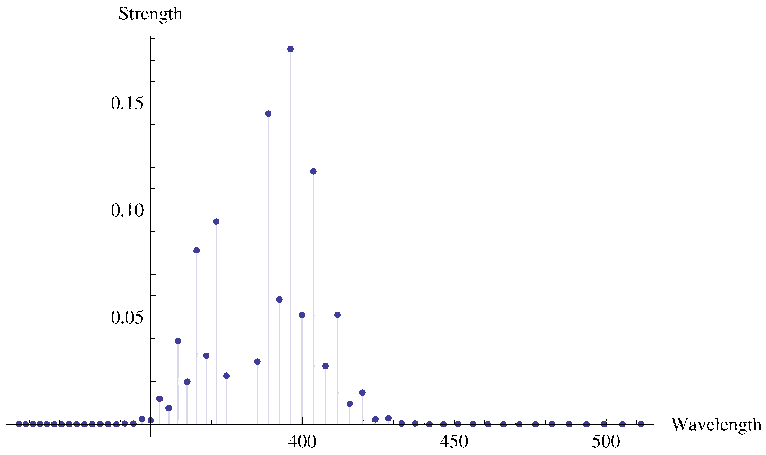

Figure 27: The Raman spectrum of H_2 for 380nm at a temperature of 2000K.

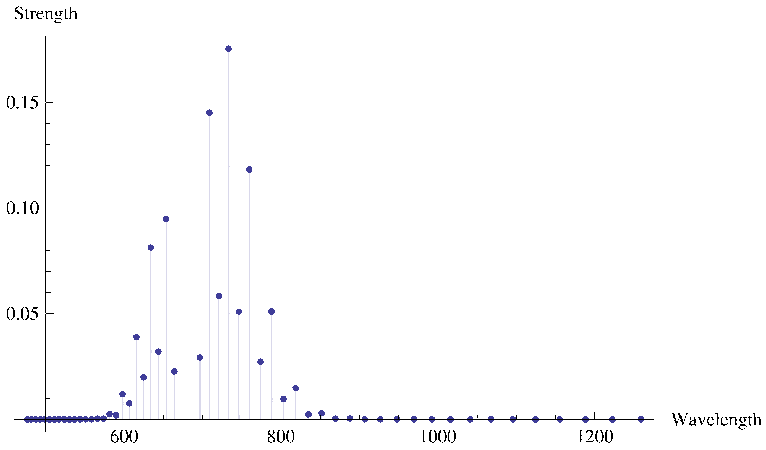

Figure 28: The Raman spectrum of H_2 for 680nm at a temperature of 2000K.

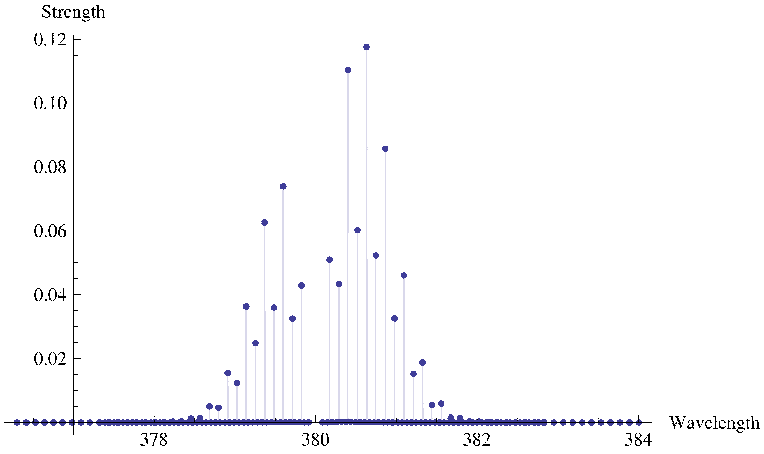

Figure 29: The Raman spectrum of N_2 for 380nm at a temperature of 100K. This is a good approximation for the atmosphere of Titan.

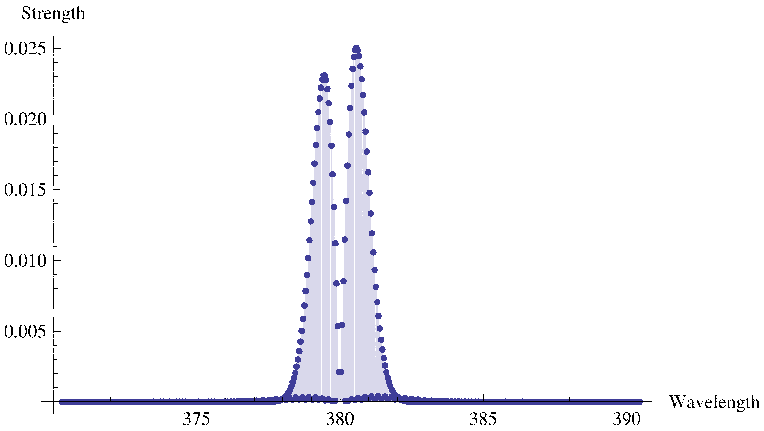

Figure 30: The Raman spectrum of CO_2 for 380nm at a temperature of 700K. This is a good approximation for the atmosphere of Venus.

C Comparison of calculated spectra

In this appendix you can find the calculated polarization spectra for H_2 and N_2 for the same values of θ, θ_0 and $\phi - \phi_0$.

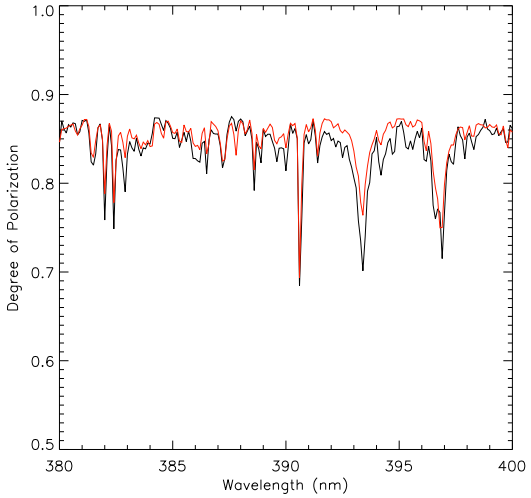

Figure 31: $\theta = 0, 1°$, $\theta_0 = 89, 9°$. Black line is H_2, red line is N_2.

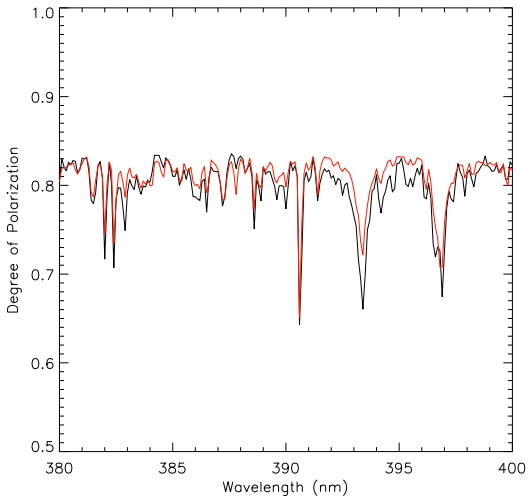

Figure 32: $\theta = 17, 46°$, $\theta_0 = 72.54°$. Black line is H_2, red line is N_2.

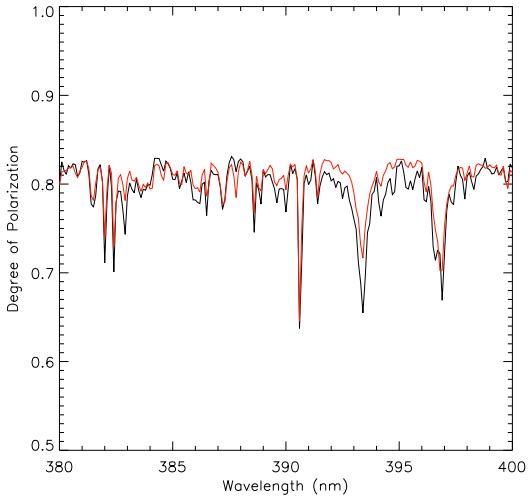

Figure 33: $\theta = 36.87°$, $\theta_0 = 53.13°$. Black line is H_2, red line is N_2.

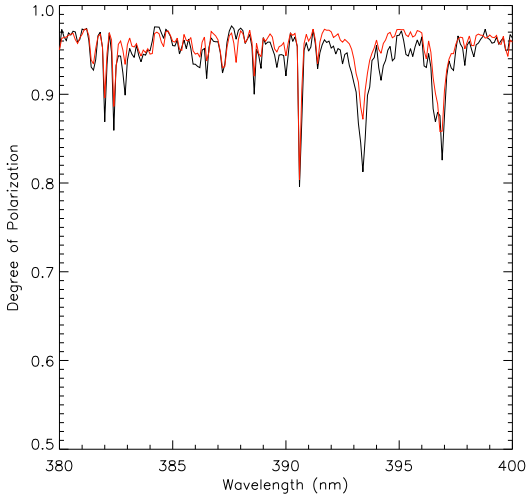

Figure 34: $\theta = 89,9°$, $\theta_0 = 0.1°$. Black line is H_2, red line is N_2.

D Integrated spectra

in this appendix you can find figure similar to figure 15 for $0° \leq \alpha \leq 330°$, $\alpha = 360°$ is not included because this is exactly the same as $\alpha = 0°$.

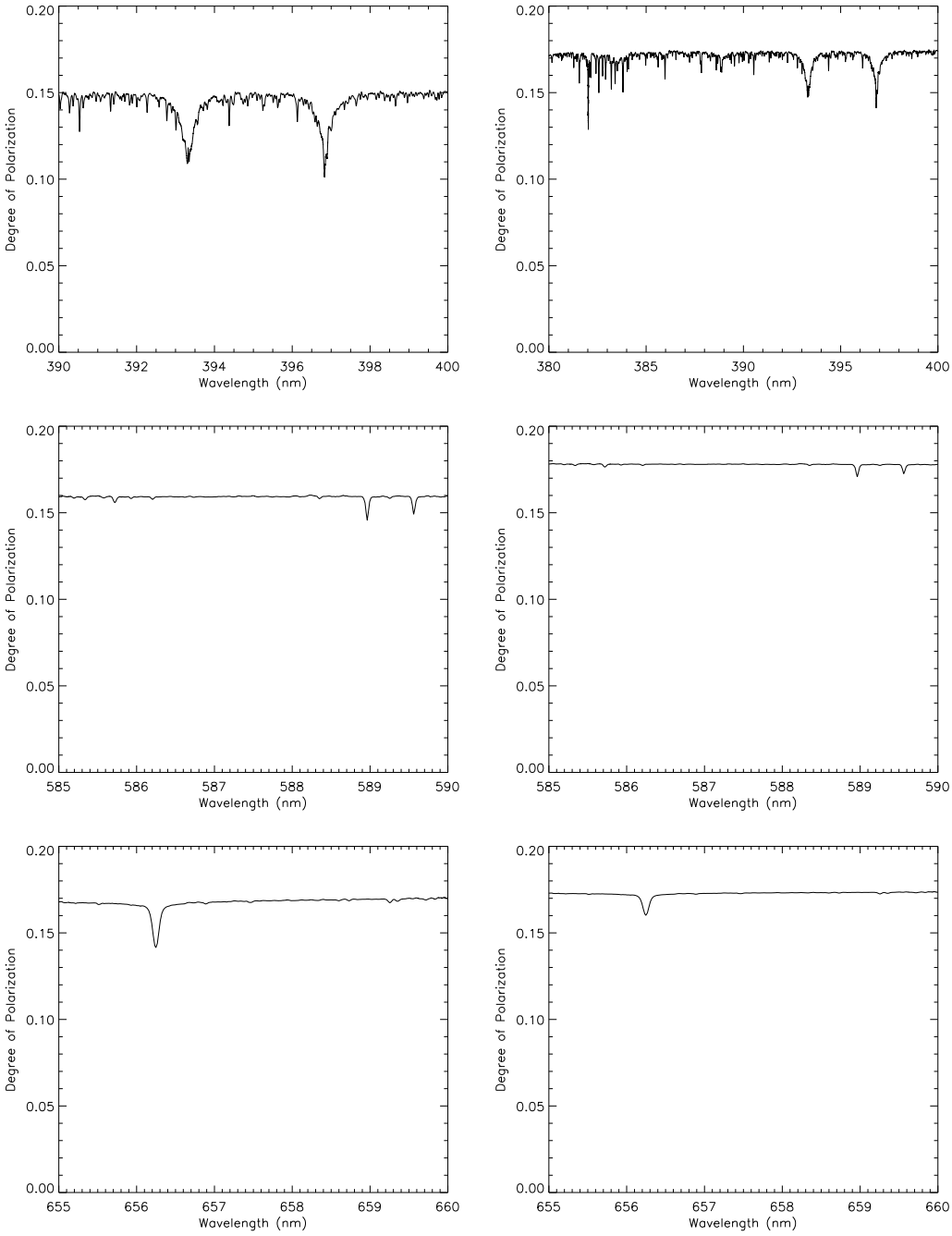

Figure 35: The polarization spectrum of just the planet (left) and the combination of planet and star (right) for the wavelength region near some of the Fraunhofer lines. First row: calcium-H (396.8nm) and calcium-K (393.4nm) lines, second row: sodium-D lines (589.6nm and 589.0nm), third row: H-α (656.3nm). $\alpha = 0°$, $i = 45°$.

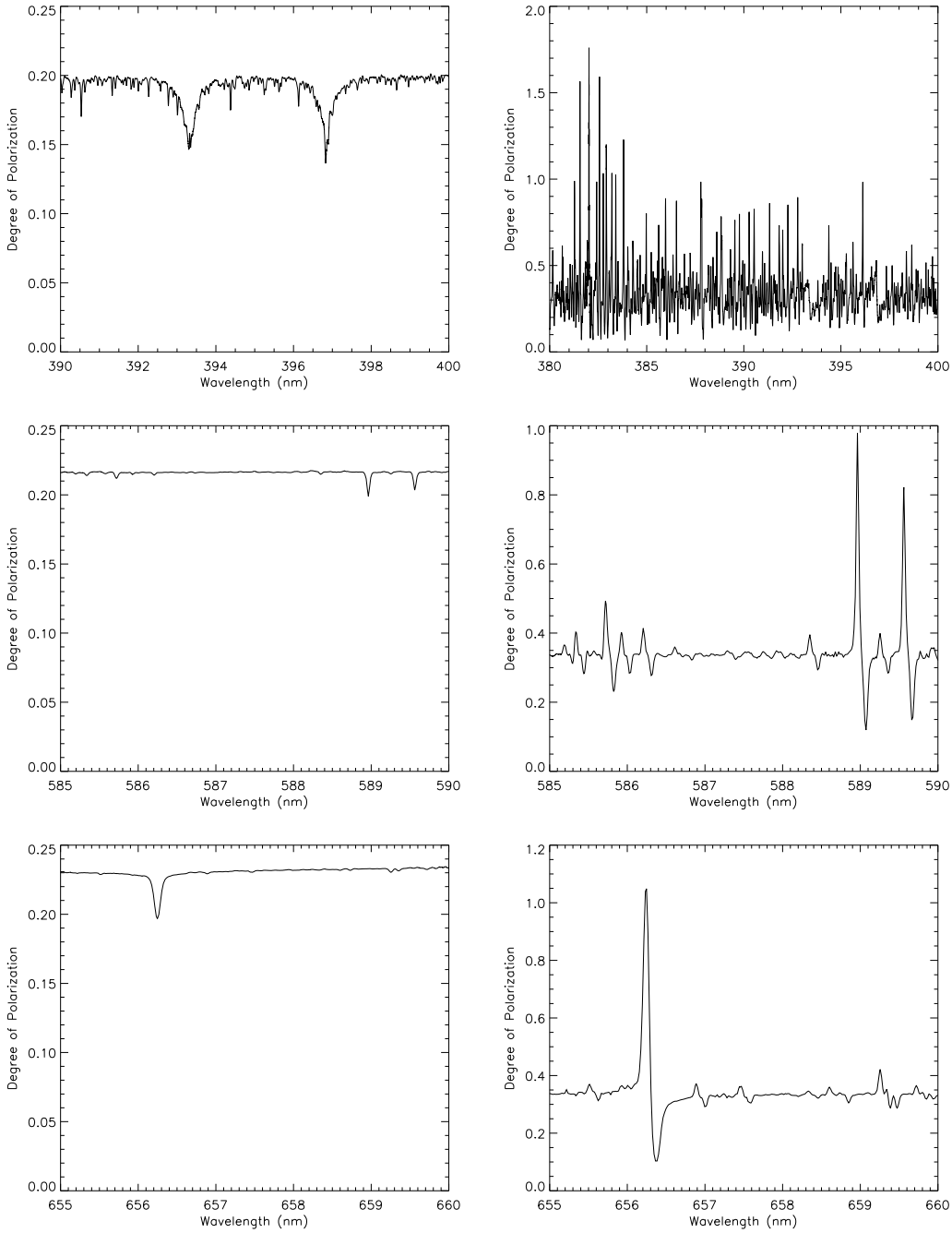

Figure 36: Same as figure 35, except $\alpha = 30°$.

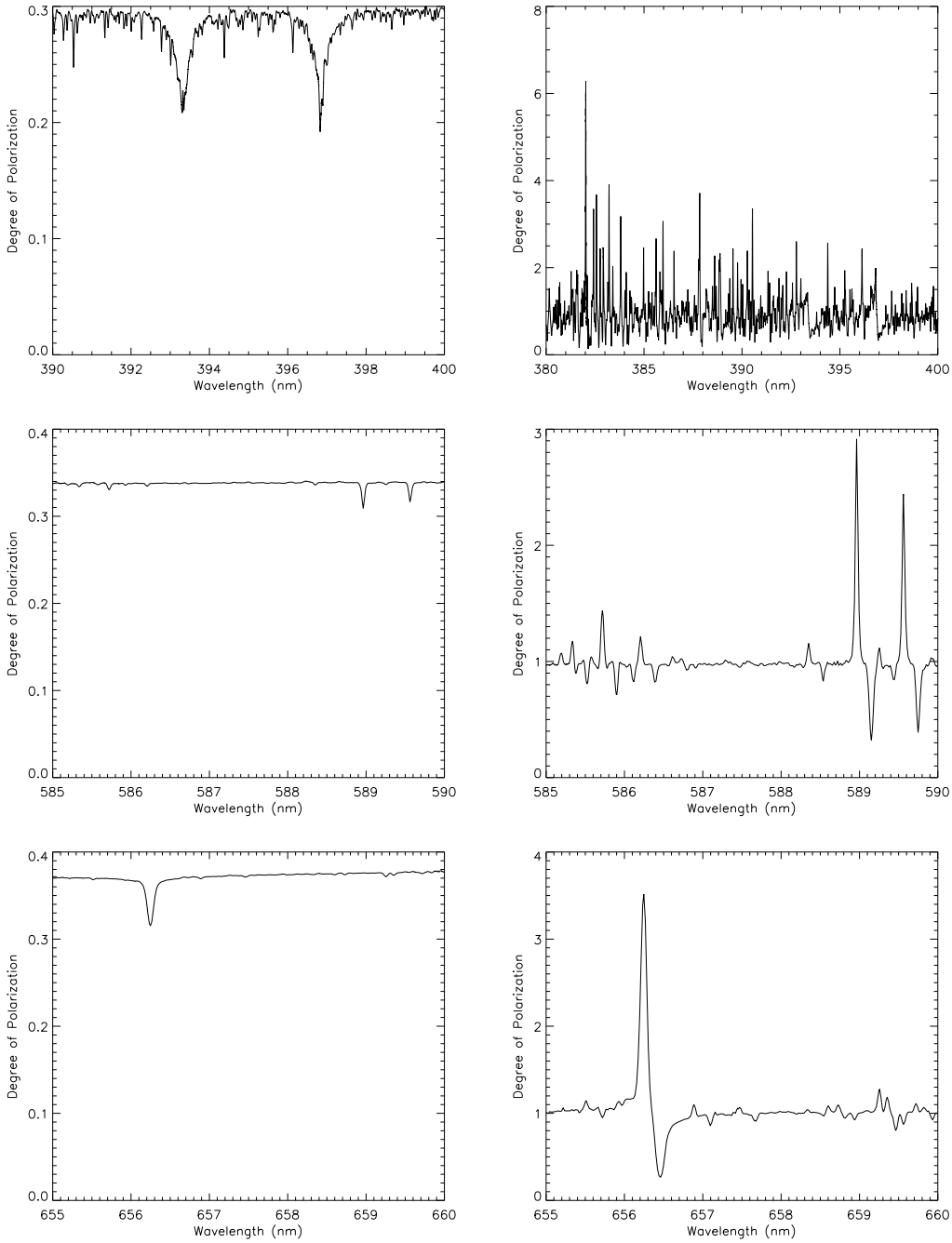

Figure 37: Same as figure 35, except $\alpha = 60°$.

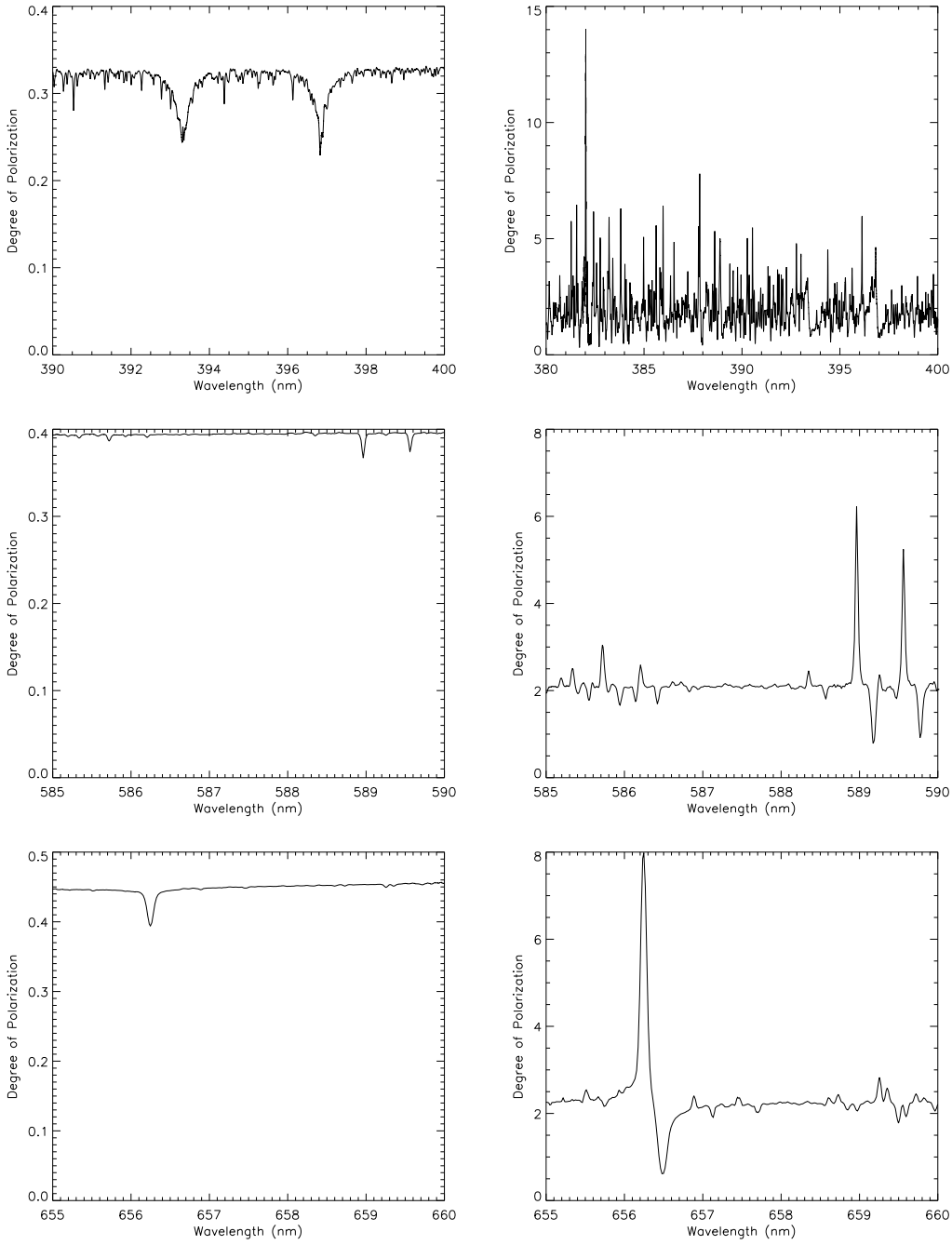

Figure 38: Same as figure 35, except $\alpha = 90°$. This figure is equal to figure 15.

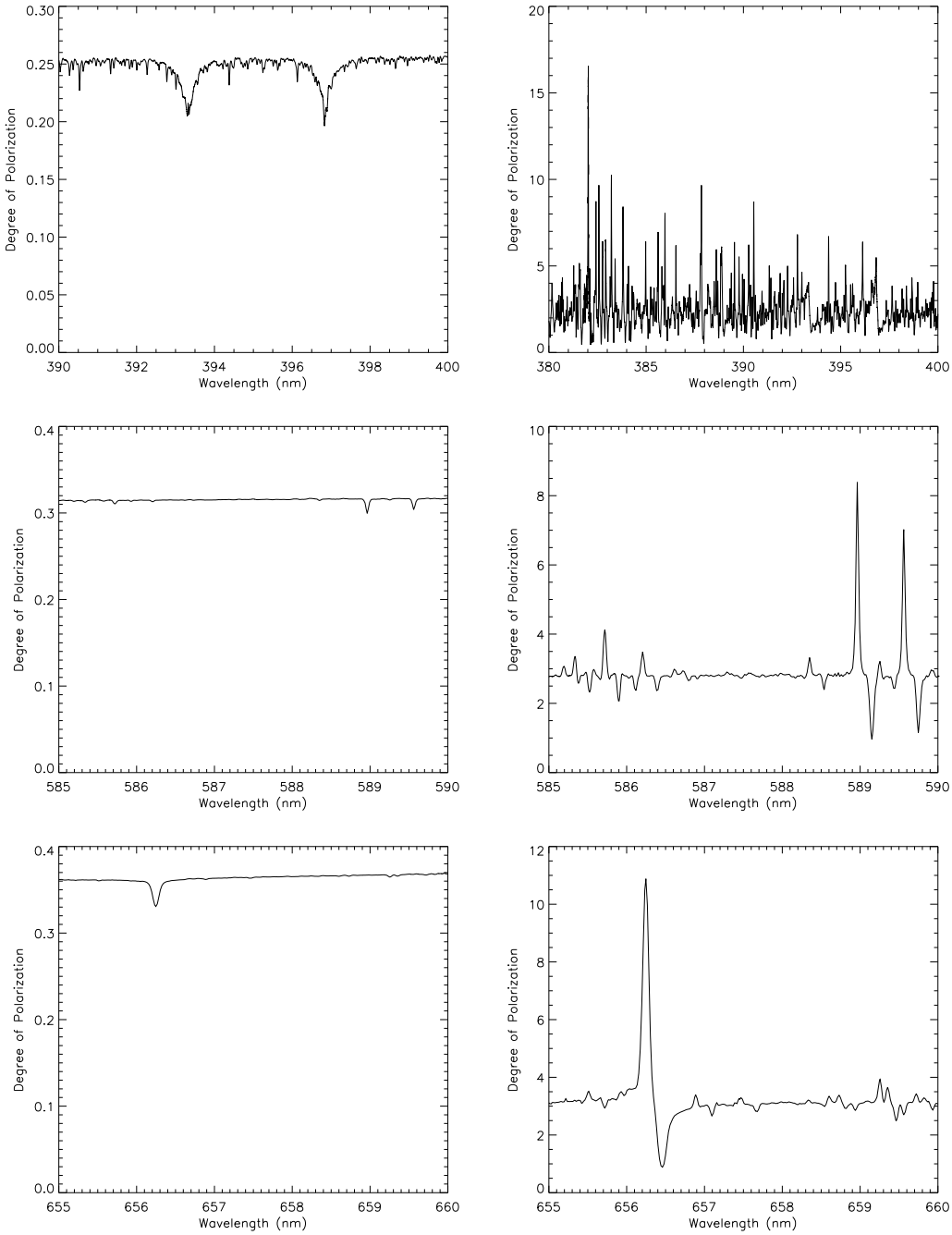

Figure 39: Same as figure 35, except $\alpha = 120°$.

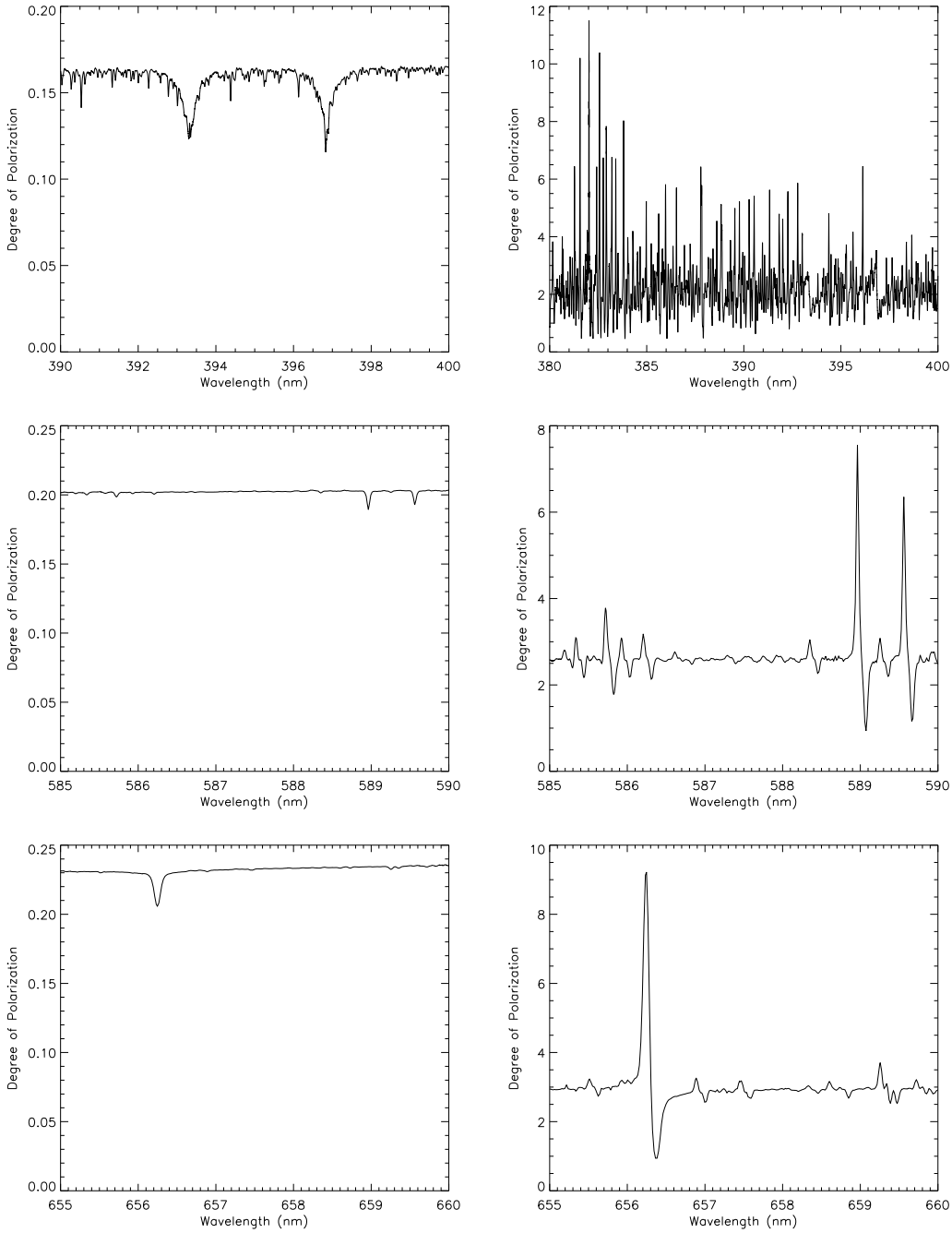

Figure 40: Same as figure 35, except $\alpha = 150°$.

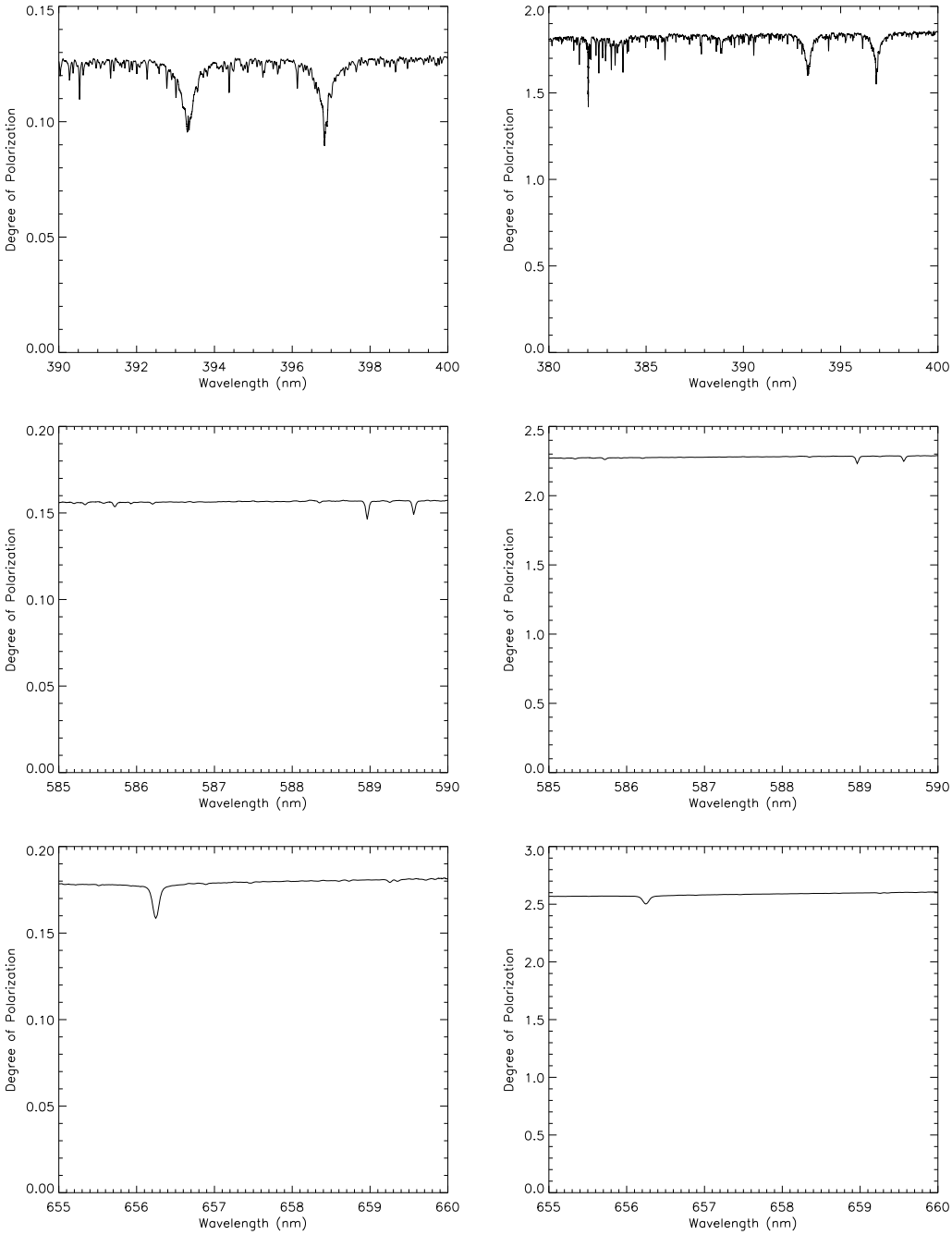

Figure 41: Same as figure 35, except $\alpha = 180°$.

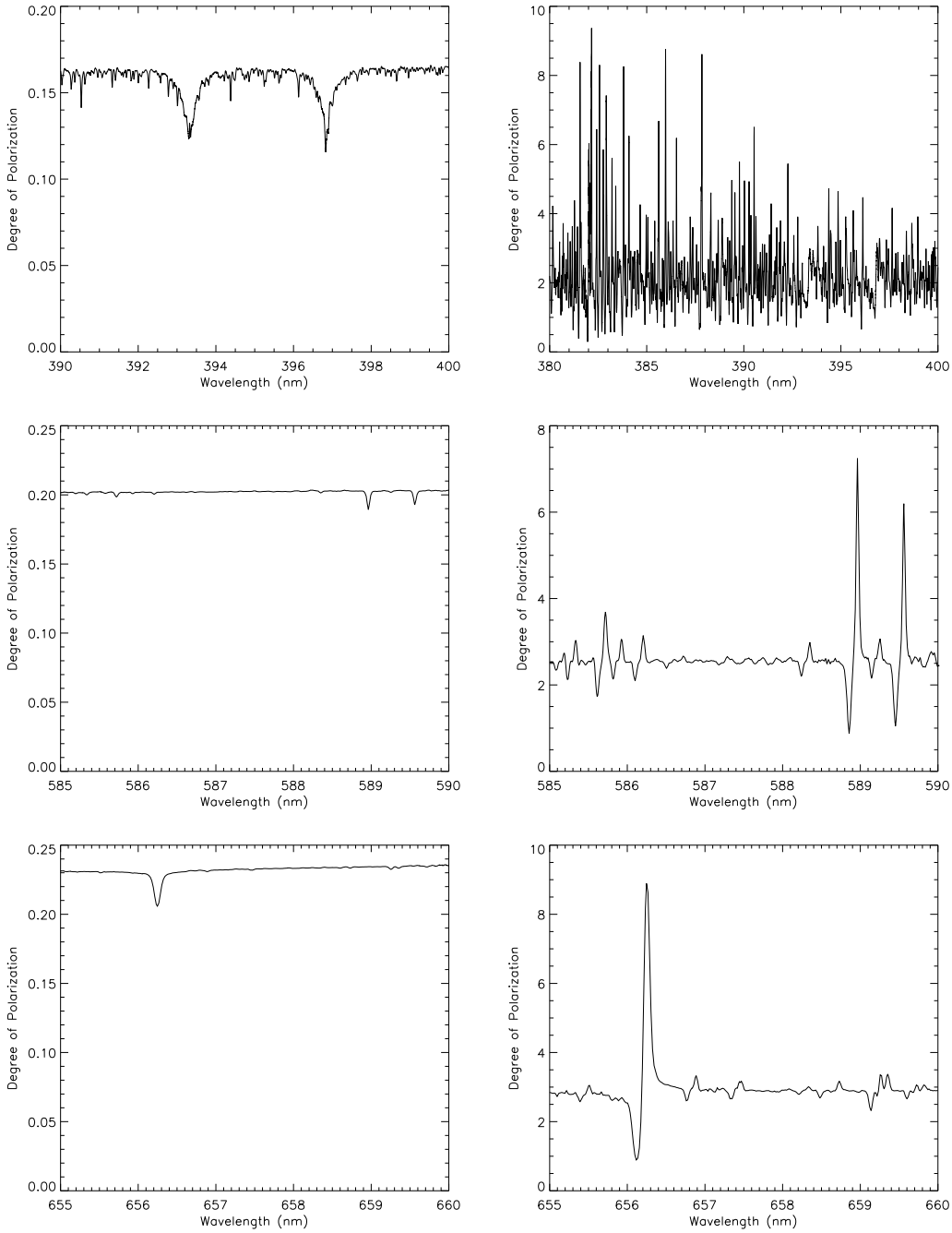

Figure 42: Same as figure 35, except $\alpha = 210°$.

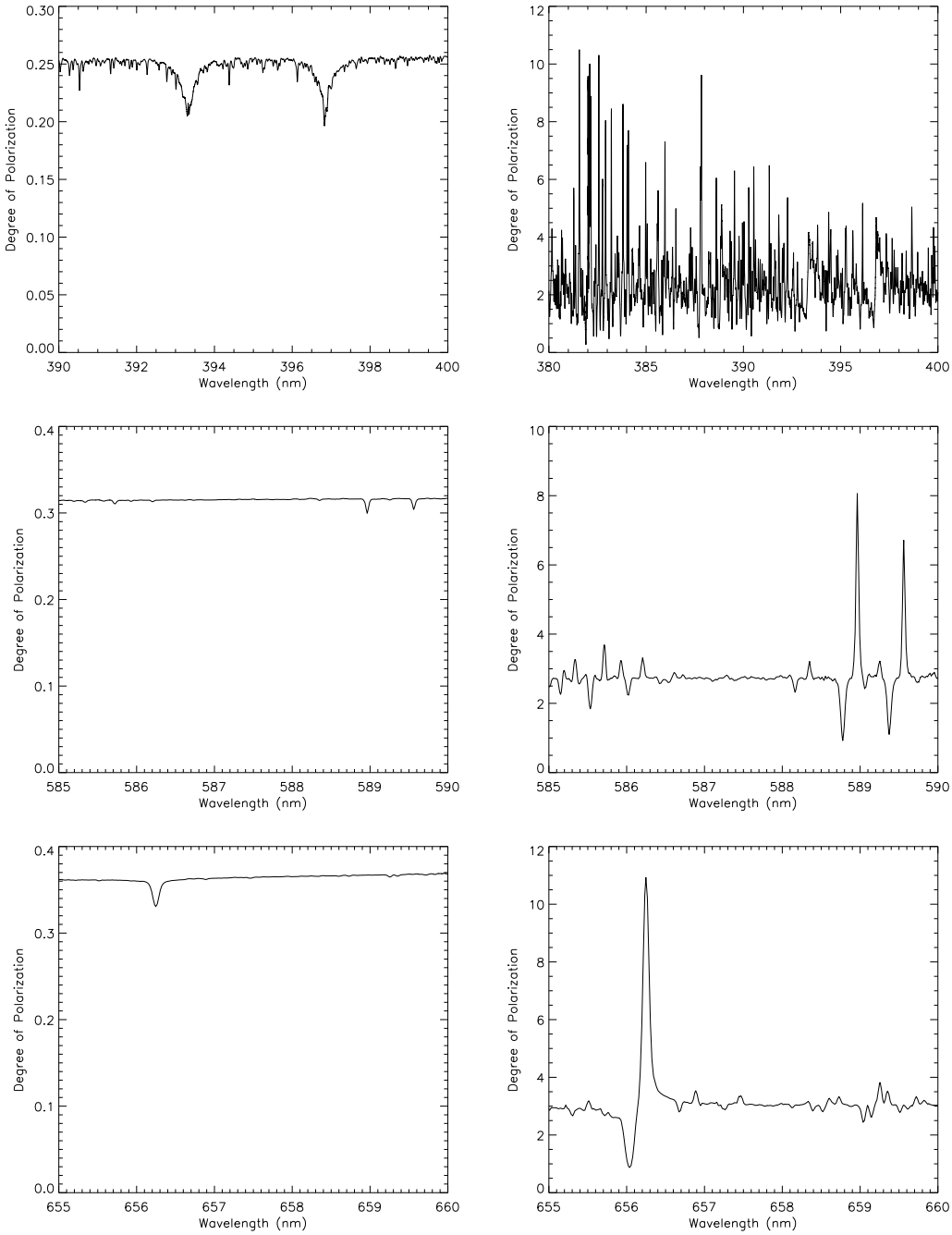

Figure 43: Same as figure 35, except $\alpha = 240°$.

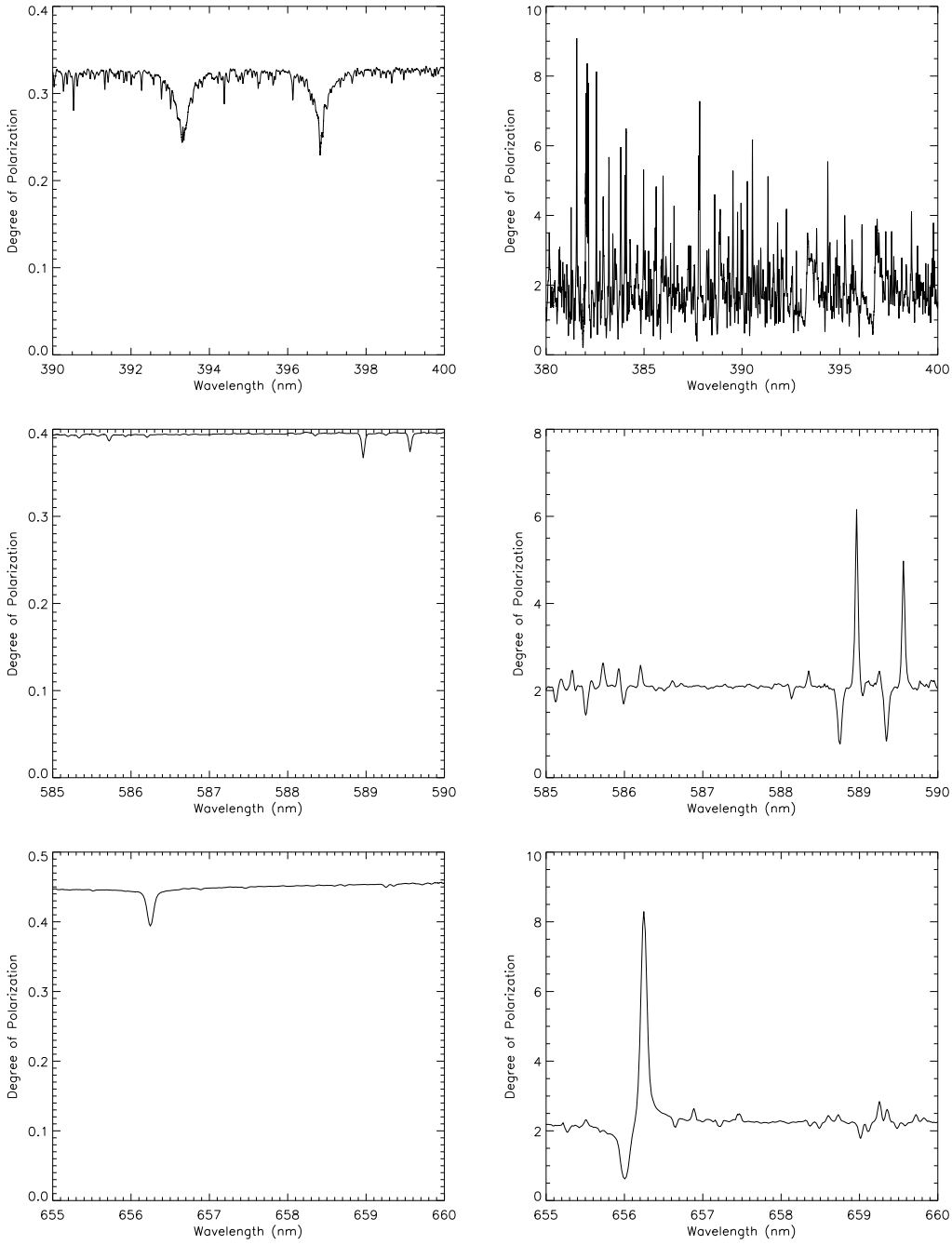

Figure 44: Same as figure 35, except $\alpha = 270°$.

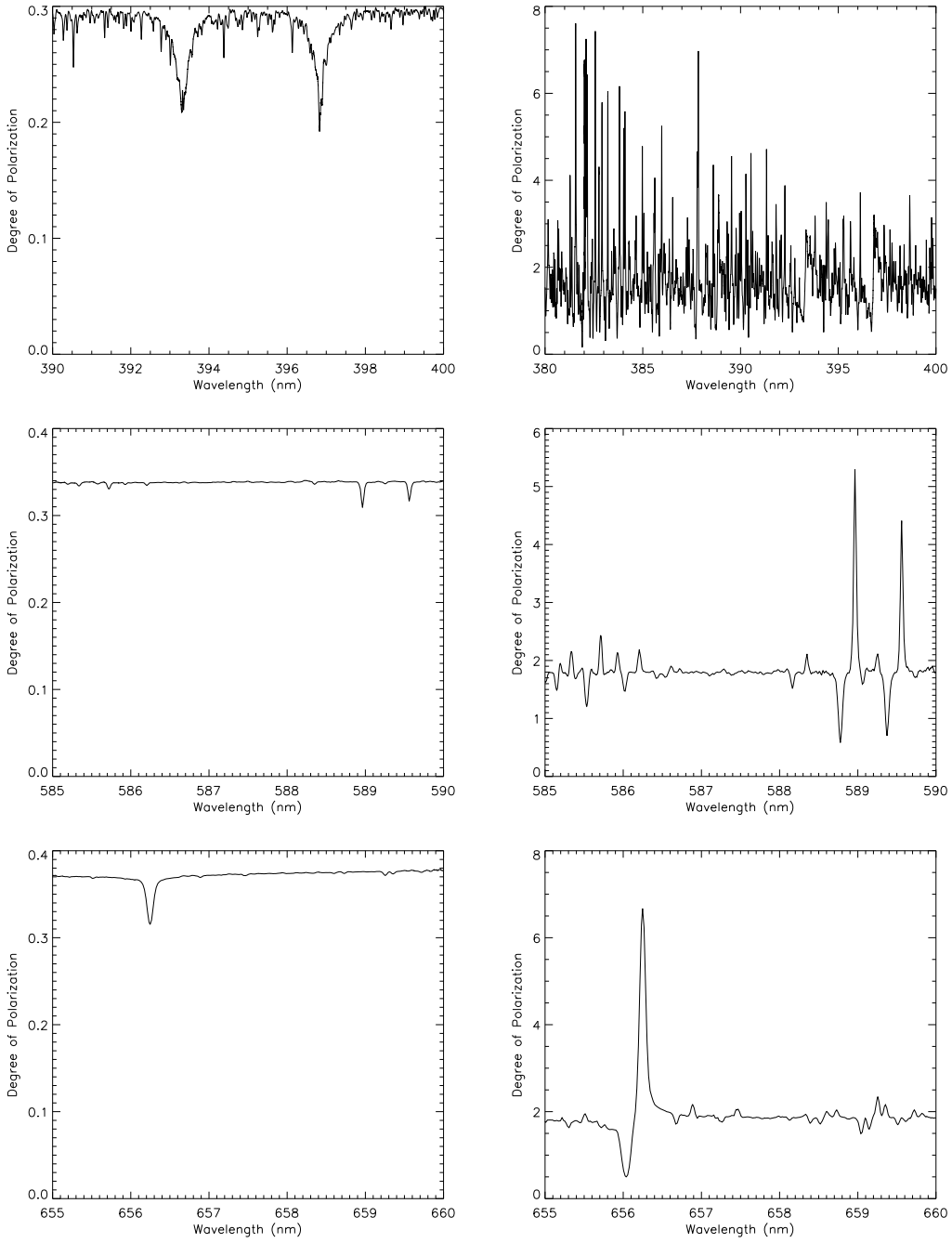

Figure 45: Same as figure 35, except $\alpha = 300°$.

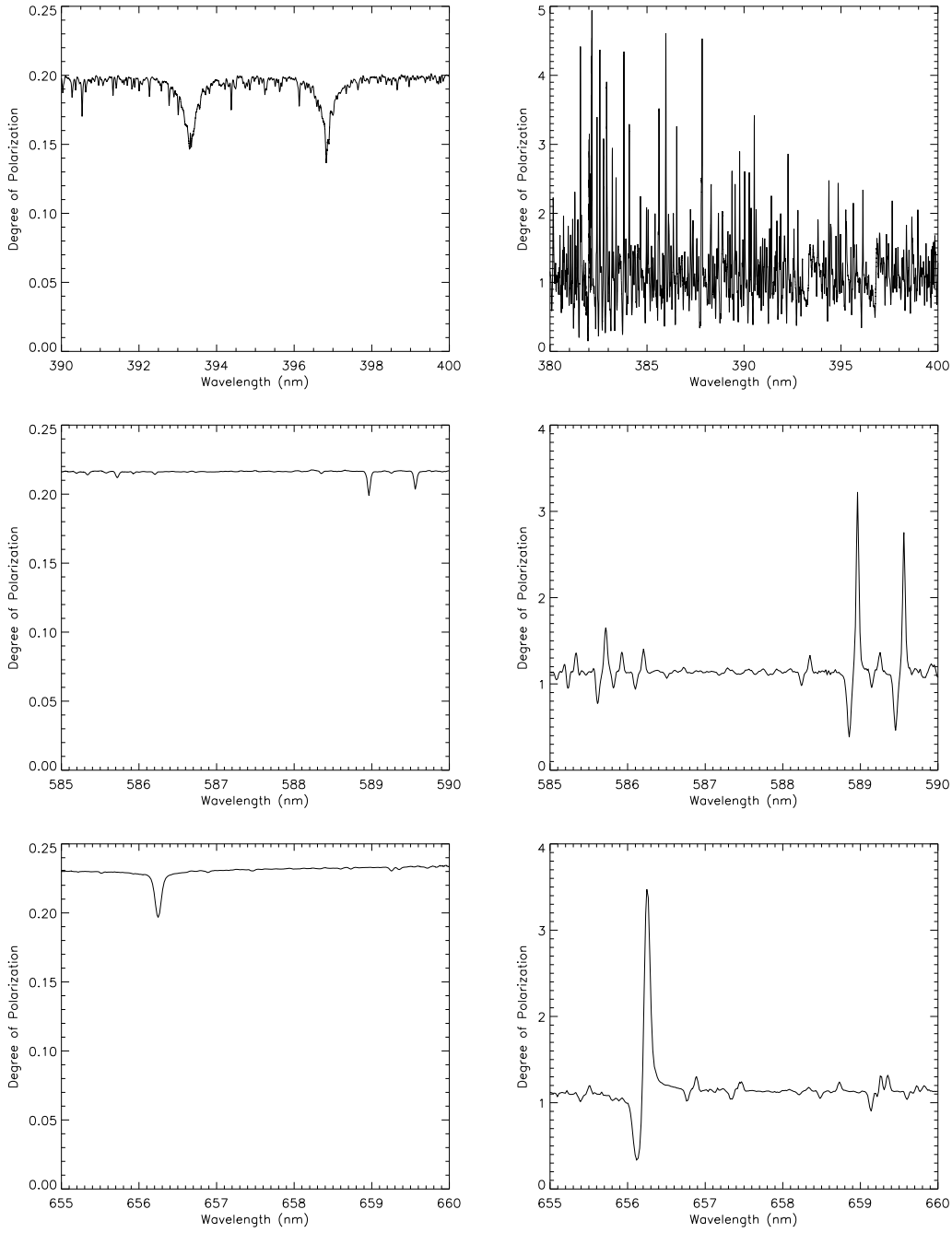

Figure 46: Same as figure 35, except $\alpha = 330°$.

References

[1] M. Mayor, D. Queloz; A Jupiter-mass companion to solar type star; 1995Natur.378..355M

[2] F. Rodler, M. Kürster, T. Henning;τ Boötis, hunting for reflected star light;2010A&A...514A..23R

[3] J.F. Grainger, J. Ring; Anomalous Fraunhofer Line Profiles; 1962Natur.193..762G

[4] J. Noxon, R.Goody; Noncoherent scattering of skylight; Atmos. Oceanic Phys., 1, 163-166, 1965

[5] D.M. Stam, I. Aben, F. Helderman; Skylight polarization spectra: Numerical simulation of the Ring effect; 2002JGRD..107.4419S

[6] Y. Betremieux, R.V. Yelle; HST Detection of H_2 Raman Scattering in the Jovian Atmosphere; 1999Icar..142..324B

[7] L.A. Sromovsky; Accurate and approximate calculations of Raman scattering in the atmosphere of Neptune; 2005Icar..173..254S

[8] A.T. Young; Rayleigh Scattering; 1981ApOpt..20..533Y

[9] M. Sneep, W.Ubachs; Direct measurement of the Rayleigh scattering cross section in various gases ;2005JQSRT..92..293S

[10] C.M. Penney, R.L. St. Peters, M. Lapp; Absolute rotational Raman cross sections for N_2, O_2 and CO_2;1974JOSA...64..712P

[11] R. Penndorf; Tables of the Refractive Index for Standard Air and the Rayleigh Scattering Coefficient for the Spectral Region between 0.2μm and 20μm and Their Application to Atmospheric Gases; 1957JOSA...47..176P

[12] S.L. Bragg, W.H. Smith, J.W. Brault; Line Positions and Strengths in the H_2 quadrupole spectrum;1982ApJ...263..999B

[13] U. Fink, T.A. Wiggins, D.H. Rank; Frequency and Intensity Measurements on the Quadrupole Spectrum of Molecular Hydrogen; 1965JMoSp..18..384F

[14] S.L. Bragg, J.W. Brault, W.H. Smith; Line Positions and Strengths the H_2 Quadrupole Spectrum; 1982ApJ...263..999B

[15] S.T. Massie, D.M. Hunten; Conversion of para and ortho Hydrogen in the Jovian Planets; 1982Icar...49..213M

[16] D.R. Bates; Rayleygh Scattering by Air; 1984P&SS...32..785B

[17] H.G. Horak; Diffuse Reflection by Planetary Atmospheres; 1950ApJ...112..445H

[18] Weisstein, Eric W. "Spherical Trigonometry." From MathWorld–A Wolfram Web Resource. http://mathworld.wolfram.com/SphericalTrigonometry.html

[19] D.M. Stam, W.A. De Rooij, G. Cornet, J.W. Hovenier; Integrating polarized light over a planetary disk applied to starlight reflected by extrasolar planets;2006A&A...452..669S

[20] H.C. van de Hulst; Multiple Light Scattering, Tables, Formulas, and Applications, Vols. 1 and 2 (New York: Academic Press); 1980

[21] C. Leigh, A. Collier Cameron, K. Horne, A. Penny, D. James; A new upper limit on the reflected starlight from τ Bootis b; 2003MNRAS.344.1271L

[22] R.P. Butler, G.W. Marcy, E.Williams, H. Hauser, P. Shirts; Three new "Pegasi 51–type" Planets; 1997ApJ...474L.115B

[23] J.W. Hovenier; Multiple Scattering of the Polarized Light in Planetary Atmospheres; 1971A&A....13....7H

[24] D.E. Jennings, J.W. Brault; The ground state of molecular hydrogen; 1983JMoSp.102..265J

[25] D.E. Jennings, S.L. Bragg, J.W. Brault; The V = 0-0 spectrum of H2; 1984ApJ...282L..85J

[26] L.V. King. (1923); On the complex anisotropic molecule in relation to the dispersion and scattering of light.; Proc. Roy.Sot. A 104, 333-357

[27] D.M. Kipping, D.S. Spiegel; Analysis of Kepler's Short-cadence Photometry for TrES-2b;2011ApJ...733...36K

[28] D.M. Kipping, G. Bakos; Detection of light from the darkest world; 2011arXiv1108.2297K (expected in MNRAS)

[29] M.E. Mickelson; Electronic Ground State Parameters for Molecular Hydrogen;1998ASPC..134..450M

[30] D.M. Stam; Polarization Spectra of Extrasolar Giant Planets; 2004ASPC..321..195S

[31] D.M. Stam; Spectropolarimetric signatures of Earth-like extrasolar planets; 2008A&A...482..989S